

ANKARA YILDIRIM BEYAZIT UNIVERSITY
GRADUATE SCHOOL OF NATURAL AND APPLIED SCIENCES

A NEW APPROACH FOR COUNTING AND SIZING THE OBJECTS: IMAGE WEIGHT SIGNAL

M.Sc. Thesis by

Zeynep YILDIZ

Department of Electronics and Communication Engineering

June, 2016

ANKARA

A NEW APPROACH FOR COUNTING AND SIZING THE OBJECTS: IMAGE WEIGHT SIGNAL

A Thesis Submitted to
the Graduate School of Natural and Applied Sciences of Ankara Yıldırım Beyazıt University
In Partial Fulfillment of the Requirements for the Degree of Master of Science in Electronics and Communication Engineering, Department of Electronics and Communication Engineering

by

Zeynep YILDIZ

June, 2016

ANKARA

M.Sc THESIS EXAMINATION RESULT FORM

We have read the thesis entitled "A NEW APPROACH FOR COUNTING AND SIZING THE OBJECTS: IMAGE WEIGHT SIGNAL" completed by Zeynep YILDIZ under supervision of Assoc. Prof. Dr. İlyas ÇANKAYA and we certify that in our opinion it is fully adequate, in scope and in quality, as a thesis for the degree of Master of Science.

Assoc. Prof. Dr. İlyas ÇANKAYA

(Supervisor)

Prof. Dr. Recep DEMİRCİ

(Jury Member)

Assist. Prof. Dr. Hilal KAYA

(Jury Member)

Prof. Dr. Fatih V. ÇELEBİ

(Director)

Graduate School of Natural and Applied Sciences

DECLARATION OF ETHICS

For this thesis I prepared in accordance with Ankara Yıldırım Beyazıt University, Graduate School Of Natural And Applied Sciences, Thesis Writing Rules, I announce that;

- I obtained data, information and documents, which I presented in the thesis, in the framework of academic and ethical rules,
- I presented all information, documents, evaluation and results in according to scientific ethics and morality rules,
- I gave references of all works, which I took advantage in thesis study, with refering appropriately,
- I didn't make any changes on the used data,
- The study I presented in this thesis is original,

I declare that I accepted all right losses that may arise against me in otherwise a situation.

A NEW APPROACH FOR COUNTING AND SIZING THE OBJECTS: IMAGE WEIGHT SIGNAL

ABSTRACT

Image analysis is general name of technique or techniques whose input is an image, and also output is a processed image and various quantitative parameters belong to the image. Medical image analysis is one of the most important branches of the image analysis. This field offers support and guidance to radiology specialists on the diagnosis, treatment plan and the follow-up phases of the treatments, based on the results that it produces with image analysis techniques. Among processing works of the medical images, it is the majority that ones aim to separate the specific regions from others in the image. However in the medical image analysis, one of the most difficult duties is the extraction of features and quantitative parameters about those specific regions from the image. As the reason of this difficulty, it may be given that the regions of interest and desired feature extraction have different size and shapes, therefore analysis techniques need the preliminary definitions about the regions. Because of this difficulty, analysis techniques are insufficient on obtaining quantitative parameters belong to decomposed regions in the medical image. The main aim of this study is to develop an analysis technique (Image Weight Signal (IWS)) that calculate the number and area information of the regions or objects of interest. In addition to developed analysis technique, its applications on the medical lung CT images are aimed.

Image analysis techniques are developed and applied with a paradigm known as computer-aided diagnosis (CAD) to simplify radiologic definitions. In the scope of this thesis, CAD application framework that will make it possible to measure the number and area information of the diseased regions in the medical images has been formed. This CAD application designed in Matlab GUI allows to practise with putting medical image processing and analysis methods into a sequence, supports radiology specialists on the diagnosis, treatment planning and follow-up with the help of produced information and offers the user convenience for making it possible to be used by not only engineers, but also field professionals.

Keywords: Medical Image Analysis, Image Weight Signal (IWS), The Cancer Imaging Archive (TCIA), MATLAB GUI.

OBJELERİN SAYIMI VE BOYUTLANDIRILMASI İÇİN YENİ BİR YAKLAŞIM: GÖRÜNTÜ AĞIRLIK SİNYALİ

ÖZET

Görüntü analizi genel olarak girdisi bir resim olan, çıktısı da yine işlenmiş bir resim ve bu resimlere ait çeşitli nicel parametreler olan teknik ya da tekniklerin genel ismidir. Görüntü analizinin en önemli dallarından birisi olan tıbbi görüntü analizi, görüntü hakkında analiz teknikleri ile ürettiği sonuçlar doğrultusunda radyoloji uzmanlarına tanı, tedavi planı ve uygulanan tedavinin takibi aşamalarında yardımcı ve yol gösterici olmaktadır. Tıbbi görüntülerin işlenmesi çalışmaları arasında, görüntüdeki belli bölgeleri ayrıştırmayı amaçlayanlar çoğunluktadır. Halbuki, görüntü analizinde en zorlu görevlerden birisi, görüntülerden özellik çıkarmaktır. Bu zorluğun kaynağı olarak da özellik parametresi çıkarılması istenen ve ilgilenilen bölgelerin farklı boyut ve şekilde olması, bu sebeple analiz tekniklerinin bölgeler hakkında ön tanımlamalara gereksinim duyması gösterilebilir. Bu zorluklar sebebiyle tıbbi görüntülerde ayrıştırılmış bölgelere ait nicel parametrelerin elde edilmesi konusundaki analiz teknikleri yetersiz kalmaktadır. Bu tez çalışmasının ana amacı, ilgilenilen bölgelerin ya da objelerin sayısının ve alan bilgilerinin hesaplanmasına yönelik bir analiz tekniği (Image Weight Signal (IWS)) geliştirmektir. Ayrıca geliştirilen analiz yönteminin, tıbbi akciğer CT görüntüleri üzerinde uygulanması da hedeflenmektedir.

Görüntü analizi teknikleri, computer-aided diagnosis (CAD) olarak bilinen bir paradigma ile radyolojik tanımlamaları kolaylaştırmak için geliştirilmektedir. Bu tez çalışması kapsamında, radyolojik tıbbi görüntülerde, geliştirilen IWS analiz yöntemi ile hastalıklı bölgelerin alan bilgilerinin ölçümlenmesini mümkün kılacak bir CAD uygulama çatısı meydana getirilmiştir. MATLAB GUI ortamında tasarlanan CAD uygulaması, tıbbi görüntü işleme ve analiz yöntemlerini sıraya koyarak uygulamaya imkan vermekte, üretilen bilgiler yardımıyla radyoloji uzmanlarının tanı, tedavi planı ve tedavi takibini desteklemekte ve mühendis olmayan alan profesyonelleri tarafından da kullanılmasını mümkün kılmak için kullanıcı kolaylığı sunmaktadır.

Anahtar sözcükler: Tıbbi Görüntü Analizi, Görüntü Ağırlık Sinyali (GAS), The Cancer Imaging Archive (TCIA), MATLAB GUI.

ACKNOWLEDGMENTS

I would like to take this opportunity to thank my tutor and supervisor Assoc. Prof. İlyas ÇANKAYA and for his support, guidance, encouragement and enthusiasm he showed from the initial stages to the end of the project. It has been an honor and a pleasure for me to work with him.

I would also like to express my gratitude to my father for his support during all my life, especially in my education.

Finally, I would like to thank my husband, my family, mother and father, for being with me all the way.

Without you, I wouldn't be here.

Zeynep YILDIZ 2016, 01 June

CONTENTS

M.Sc THESIS EXAMINATION RESULT FORM ..... **ii**
DECLARATION OF ETHICS ..... **iii**
ABSTRACT ..... **iv**
ÖZET ..... **vi**
ACKNOWLEDGMENTS ..... **viii**
CONTENTS ..... **ix**
ABBREVATIONS ..... **xi**
LIST OF TABLES ..... **xii**
LIST OF FIGURES ..... **xiii**

CHAPTER 1 – INTRODUCTION **1**
1.1 Objective of the Thesis 2
1.2 Outline of the Thesis 4

CHAPTER 2 – BACKGROUND FOR IMAGE PROCESSING **5**
2.1 Image and Digital Image 5
2.2 Image Types 7
2.3 Image Processing 9
2.3.1 Filtering 9
2.3.1.1 Spatial Smoothing Filters 10
2.3.1.2 Spatial Sharpening Filters 14
2.3.2 Morphological Operations 16
2.3.2.1 Mathematical Morphology 17
2.3.2.2 Morphological Operators 17
2.3.3 Segmentation 21
2.3.3.1 Thresholding 22

CHAPTER 3 – IMAGE ANALYSIS **24**
3.1 Blob Analysis 25
3.2 Hough Transform 26
3.3 Connected Component Analysis 28

3.4 Image Weight Signal 29

CHAPTER 4 – COMPUTED TOMOGRAPHY IMAGING TECHNIQUE IN BIOMEDICAL 44

4.1 Computed Tomography (CT) 44

4.2 The Development of CT Devices 45

4.3 The Principle of CT Device 45

4.4 CT Image Representation and Parameters 47

4.5 CT's Generations 49

4.6 In Clinical Uses of CT Devices 52

4.7 CT's Clinical Advantages 52

4.8 CT's Clinical Disadvantages 53

CHAPTER 5 – APPLICATION OF IWS ON BIOMEDICAL IMAGES 54

5.1 Application of IWS for Lung Nodules in CT Images 54

5.2 Methodology of the Application 55

5.2.1 Detection and Extraction of Lung Nodules 57

5.2.2 Counting, Sizing and Classification of Lung Nodules 60

5.3 Application of Graphical User Interface 65

CHAPTER 6 – CONCLUSIONS AND FUTURE WORKS 73

REFERENCES 77

BIOGRAPHY 85

ABBREVATIONS

ADC	:	Analog to Digital Converter
CAD	:	Computer-Aided Diagnosis
CT	:	Computed Tomography
GAS	:	Görüntü Ağırlık Sinyali
GUI	:	Graphical User Interface
HU	:	Hounsfield Unit
IWS	:	Image Weight Signal
KNN	:	K- Nearest Neighbour
MATLAB	:	Matrix Laboratory
SE	:	Structuring Element
SVM	:	Support Vector Machine
TCIA	:	The Cancer Imaging Archive

LIST OF TABLES

Table 4.1 The HU values of common body substances 48

Table 5.1 Steps of pre-processing 58

Table 6.1 Classification performance measures 74

LIST OF FIGURES

Figure 2.1 Digital image conversion from analog image 5

Figure 2.2 Digitization of an analog image. The pixel at coordinates [*m*=19, *n*=25] has the integer brightness value of 171 6

Figure 2.3 A grayscale image in the uint8 class and pixels' brightness values for a small image part 7

Figure 2.4 Flower image along with its R, G and B components (a) RGB image, (b) R component, (c) G component and (d) B component 8

Figure 2.5 Filtered images of the flower image using average filter with mask size (a) 3x3, (b) 5x5, (c) 11x11 11

Figure 2.6 Filtered images of flower image using Gaussian filter with different variances (a) 0.01, (b) 0.5, (c) 0.99 for mask size 3x3 12

Figure 2.7 The illustration of a median value calculation 13

Figure 2.8 (a) The flower image which salt and pepper noise was added on; (b) filtered image using median filter with different mask sizes 3x3, (c) 5x5 and (d) 11x11 13

Figure 2.9 (a) Filtered image using blurring filter with mask size 5; (b) filtered image using motion filter with two parameters of 35 and 50 14

Figure 2.10 Sharpening process (a) the flower image; (b) extraction of the details with high frequency from the image with high pass filter; (c) sharpened image obtained with placement of the details on the image 15

Figure 2.11 Filtered images using (a) unsharp filter; (b) prewitt filter; and (c) sobel filter 16

Figure 2.12 Basic Boolean logical operators: (a) binary image A; (b) binary image B; (c) A AND B; (d) A OR B; (e) A XOR B; (f) NOT A 17

Figure 2.13 Example of morphological dilation. (a) A binary input image; (b) A line structure element with mask parameter 9 and 45; (c) Dilated image of (a) by SE (b); (d) After twice dilation by SE (b); (e) After three times dilation by SE (b); (f) An octagon structure element with mask parameter 3; (g) Dilated image of (a) by SE (f); (h) After twice dilation by SE (f); (i) After three times dilation by (f) 18

Figure 2.14 Example of morphological erosion. (a) A binary input image; (b) A line structure element with mask parameter 9 and 45; (c) Eroded image of (a) by SE (b); (d) After twice erosion by SE (b); (e) After three times erosion by SE (b); (f) An octagon structure element with mask parameter 3; (g) Eroded image of (a) by SE (f); (h) After twice erosion by SE (f); (i) After three times erosion by (f) 19

Figure 2.15 Opening of a gray-scale image with an 7x7 octagonal SE; (a) a gray-scale image; (b) eroded image by an octagonal SE; (c) dilated image by the same octagonal SE after erosion 20

Figure 2.16 Closing of a gray-scale image with an 7x7 octagonal SE; (a) a gray-scale image; (b) dilated image by an octagonal SE; (c) eroded image by the same octagonal SE after dilation 21

Figure 2.17 Application of Otsu Threshold segmentation; (a) gray level image and (b) segmented image with the treshold value of 190 23

Figure 3.1 An example application of object counting using Blob analysis method (a) a binary digital image as input; (b) the output image whose objects are labeled to a unique level; (c) the algorithm's result giving the counted number of objects..... 26

Figure 3.2 An example application of object counting using circular Hough Transform (a) a binary digital image as input; (b) the output image whose objects are bounded with blue circles and their centers are marked with red plus sign..... 27

Figure 3.3 An example application of object counting using Connected Component method (a) a binary digital image as input; (b) the algorithm's result giving the counted number of objects depend on the connectivity parameter 28

Figure 3.4 The example images whose objects are located on (a) horizontal plane for IWS with horizontal scanning, (b) vertical plane for IWS with vertical scanning, and (c) diagonal plane for IWS with both scanning types 30

Figure 3.5 An application of Algorithm 1 on (a) black-white *im* image and (b) obtained IWS function graph with vertical scanning as the result of the algorithm.. 33

Figure 3.6 Derivative function graph of IWS and detected decreased sections on derivative function as a result of Algorithm 2 35

Figure 3.7 As results of Algorithm 3, (a) obtained region matrix with decomposition decreased sections and (b) local minimum points of decomposed regions 37

Figure 3.8 Display graph of local minimum points representing the objects on the derivative function's decreased sections..... 37

Figure 3.9 Superposition graph of the local minimum points on the IWS with vertical scanning..... 38

Figure 3.10 Calculated area information of the objects 40

Figure 3.11 An application of the IWS on (a) the black-white image; and as a result, obtained (b) superposition graph of the local minimum points representing objects on the IWS; and (c) calculated area information of the objects..... 41

Figure 3.12 An application of IWS and Blob analysis on (a) the array images whose sizes are increasing at each step and (b) the time comparison graph of both counting and sizing techniques on the image array 42

Figure 3.13 An application of the IWS on (a) the black-white rice image; and as a result, (b) obtained superposition graph of the local minimum points representing objects on the IWS 43

Figure 4.1 The basic elements and operations of the CT system 46

Figure 4.2 The process of "windowing", which maps a range of pixel values in window to a grayscale 49

Figure 4.3 The first generation of CT systems 49

Figure 4.4 The second generation of CT systems 50

Figure 4.5 The third generation of CT systems 51

Figure 4.6 The fourth generation of CT systems 51

Figure 5.1 Flow chart for steps and processes of application 56

Figure 5.2 Filtering process of the bronchial tubes in the the right and left lung images obtained with pre-processing steps from input CT image 60

Figure 5.3 The IWS and results of IWS analysis on the (a) lung CT image with nodules by the (b) vertical scanning and (c) horizontal scanning 62

Figure 5.4 (a) Vertical alignment and (b) horizontal alignment of the detected nodules 63

Figure 5.5 The IWS and results of IWS analysis on the (a) lung CT image with nodules by the (b) horizontal scanning and (c) vertical scanning 64

Figure 5.6 (a) Horizontal alignment and (b) vertical alignment of the detected nodules 65

Figure 5.7 The IWS and results of IWS analysis on the lung CT image without nodule for right and left lungs 65

Figure 5.8 Designed graphical user interface for CAD system 66

Figure 5.9 Process panel and its subsections 67

Figure 5.10 Patient selection by pop-up menu 68

Figure 5.11 Lung mask image on the figure window opened by 1.b push button 68

Figure 5.12 Usage of slider and its effects on the image 69

Figure 5.13 Presentation of CT image on section 2 70

Figure 5.14 Presentation of pre-processed and separated lungs' images on the section 3 71

Figure 5.15 Presentation of IWS on the section 4 71

Figure 5.16 Presentation of quantitative parameters on the section 5.a 72

Figure 5.17 Presentation of quantitative parameters on the section 5.b 72

Figure 6.1 An example of the wrong maske production 75

CHAPTER 1

INTRODUCTION

Digital images' place, effect and function on the modern society, science, technology and art is enormous. Because of the fact that it has found a place in almost every field, image processing and analysis have become a critical area. Image analysis is an interdisciplinary topic which is used in the microscopy, astronomy, medical imaging, computer vision, geology and many other areas, and developments involving really many disciplines formed [1-6].

Image analysis studies have been ongoing for many years in parallel to the development of imaging techniques, and increased its diversity in order to answer need. In this area, one of the most critical and important study subjects is the medical image analysis topic. Biomedical field in which interest increased and researches gained speed in the recent years has many amazing developments in terms of both used devices and processing of images obtained from these devices, and also continue to become an inspiration to many studies [7-10]. Although devices are at the forefront in the biomedical field, it has also great importance how do images obtained from these devices process, how to configure, how to make consistent with each other. Hence, digital image analysis process constitutes an important work field in the biomedical area.

The range of the image function system consists of low, medium and high evolution. Low level of evolution; includes filters aimed at noise reduction and improving image or basic operations such as contrast adjustment. In this level, inputs and outputs are images. Medium level of evolution; includes proposals such as decomposition (segmentation of the specific regions or objects), image registration and comparison. In this level, inputs are images and also outputs are images whose intelligibility is enhanced or which carries similarity properties of pixels. Low level of evolution are functions such as region/object recognition, shape analysis,

monitoring, classification of defined areas / objects and interpretation with the extraction of quantitative parameters belong to defined areas / objects from images. In this level, inputs are images. On the other hand, outputs are parameters, features or calculation of definition, classification, feature extraction and quantitative information. High-level contains generally analysis processing the cognitive functions reconciled with vision [8,11].

In the biomedical field, scientific research and clinical applications generally include low and medium level techniques. It is majority that analysis performed with these techniques aim the separation of specific regions such as tumor / nodules in the image [10, 12-17]. Because in the medical images, image analysis application with high level is a difficult and laborious process. The reason of this difficulty is images that are complicated and not clear on account of the complex structure of the human anatomy and a great amount of artifacts sourced from the imaging device or individual (failure to stand constant during scanning). Analysis techniques with high level in the medical images are insufficient due to these difficulties and needs increase in parallel with the development of imaging techniques.

1.1 Objective of the Thesis

In the medical image analysis, it is usually targeted to detect diseased regions such as mass or nodule, to extract from the image, to calculate the number of regions determined and to obtain quantitative measurements belonging to these regions. In the literature, many studies on the detection of the diseased regions as tumor/nodule have already been available [10,12-17]. Magdy et al. performed classification of lung into normal or cancer with detection of the nodules on the 70 different patients' lung CT images [10]. In that study, four different classification techniques were used; *K*-nearest neighbour (*K*NN), support vector machine (SVM), naïve Bayes, and linear classifiers. Similarly, Sivakumar and Chandrasekar conducted study on the detection and segmentation of the lung nodules [13]. In that study, it was aimed to develop an efficient lung nodule detection system with nodule segmentation based on Fuzzy-based clustering models and to classify using a machine learning technique called

Support Vector Machine (SVM). Unlike these mentioned studies, Joseph et al. studied on the brain MR images [17]. They proposed a segmentation application in which K-means clustering algorithm in order to detect tumors and then morphological filtering methods were used. Azhari et al. suggested a system that implements automatic tumor detection and functions of location determination on the brain MR images [14]. The presented system contains five basic steps including image acquisition, pre-processing, edge detection, modified histogram clustering and morphological processes. Besides the studies on the detection of the specific regions in the literature, analysis techniques which form an integral part of the image analysis were developed also to calculate the number of the object or regions [18-22]. Leading ones of these techniques are Blob Analysis, Hough Transform and Connected Component Analysis. However, it is still needed the analysis techniques to perform sizing process of the desired objects or regions, and to calculate quantitative parameters like area information. The main objective of this thesis study is to develop an analysis technique which is Image Weight Signal (IWS) for the calculation of the number and the area information of desired regions or objects. Furthermore, it is expected that the developed analysis method is applied on the medical images such as lung CT images.

Computer-aided diagnosis (CAD) is a very young interdisciplinary technology which combines elements of artificial intelligence, image processing and analysis for radiological images. CAD is a new and interesting health technology, which contains the medical procedures assisting the doctors for interpretation of the medical images in radiology. The radiologists need to analyze images and evaluate comprehensively in a short time. CAD systems help radiologists evaluate with highlighting the regions, which have the typical appearance in the digital images and seem as potential diseases. In scope of this thesis, it is also intended to form a CAD application framework which will make it possible to measure area information of the diseased regions with the developed IWS analysis method in the radiological medical images.

1.2 Outline of the Thesis

The following sections of the thesis are organized as follows:

In Chapter 2, a general background information about the definitions and functions situated in the basis of this thesis is presented. Initially, the definitions of image and types are given. Then, the image processing techniques, which were used for pre-processing step in the performed applications, are explained and each ones are examplified in MATLAB.

In Chapter 3, initially, an entry for image analysis is made. Then, counting methods being inspired for the development of presented method are explained. Subsequently, the necessity of the developed analysis method is discussed. Finally, the developed technique is described by mathematical expression, and sample results are presented.

In Chapter 4, CT imaging technique whose images are used in the thesis is explained. The development, physical working principles, parameters, usage areas, advantages and disadvantages of the imaging technique are given as the subtitles.

In Chapter 5, the developed application is presented and its steps are described. All steps involved in flow diagram of the application are explained in details, and the results and effects of the each step are shown on the sample images. In addition, user interface designed for the performed application is presented and each element contained is described.

In Chapter 6, which is the last section, a summary of this thesis and the results of the work carried out in the thesis are presented. Additionally, suggestions for future works to be able to be done with the developed method are given.

CHAPTER 2

BACKGROUND FOR IMAGE PROCESSING

Electronic data processing has developed incredibly fast for the last 40 years. These developments have occurred in parallel with the advances in the computer technology. Gradually decrease in the size of the computer, increase in the memory capacity and data processing speed have lead the enormous development of the image processing techniques, softwares and technologies [23].

2.1 Image and Digital Image

An image defined in the real world is considered as *im(x,y)* function representing the amplitude (the intensity, brightness) of the point at the real coordinates *(x, y)* [24]. In recent image processing applications, digital images are used mostly rather than analog images.

A digital *im*(*m*,*n*) image defined in the two-dimensional discrete space is derived by digitizing operation from the analog *im(x,y)* image defined in the two-dimensional continuous space [24]. In fact, *im*(*x*,*y*) is a function which depends on many variables such as depth(*z*), color(λ) and time(*t*). However, digital image obtained by digitizing is a function which both planar coordinates and gray level values of a continuous image are digitized [25]. The conversion of the analog image to digital image includes two important processes known as sampling and quantization [26]. The flow chart of the digitization is shown in Figure 2.1.

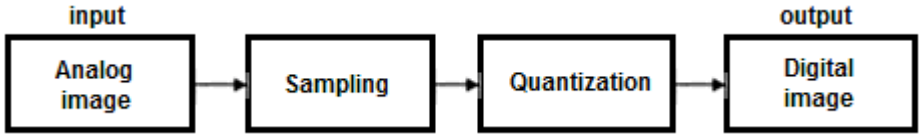

Figure 2.1 Digital image conversion from analog image

It is called image sampling that the coordinate values are digitized as the discrete values. The two-dimensional analog $im(x,y)$ image is divided into M rows and N columns with the sampling process. The intersection of a row and a column carries pixel value expressing the smallest part of the image. The values marked in the coordinate points $[m,n]$, which are sampled at the integer values as $\{m=0,1,2,\ldots,M-1\}$ and $\{n=0,1,2,\ldots,N-1\}$, represent the pixel values $im[m,n]$. It is also called image quantization that gray level values of the image are digitized as the specific discrete values [24, 25]. The digitization of an analog image is presented in Figure 2.2.

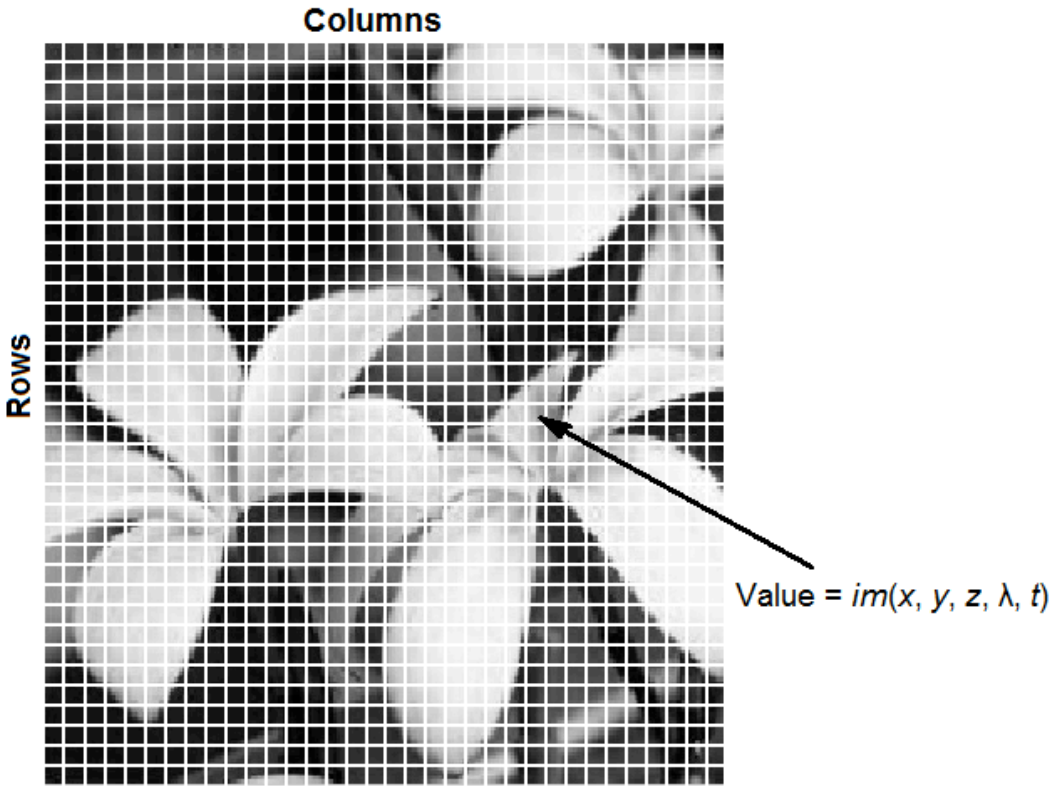

Figure 2.2 Digitization of an analog image. The pixel at coordinates [m=19, n=25] has the integer brightness value of 171

The image presented in Figure 2.2 is divided into M = 37 rows and N = 34 columns. The values assigned to pixels are the average brightness values rounded to the nearest integer value. The brightness of quantized pixel at the [m=19, n=25] coordinates is 171 value.

2.2 Image Types

A binary image is a digital image which has only two possible values for each pixel. Generally, two colors used for this type of the images are black and white. This also means that each pixel contains only a single bit, 0 or 1. In the digital image processing, binary images are produced mostly as mask or obtained as the results of the operations such as segmentation, thresholding and dithering [27].

Gray level images are matrices containing the components which represent intensity values of the pixels. In such images, each pixel carries only intensity information. This intensity information consists of only shades of gray and is diversified from black, which is the weakest brightness, to white, which is the most powerful brightness [28]. The pixels of the gray level consist of 8 bits. Possible 2^8 (256) differet values are obtained from these 8 bits. If class of image is uint8, black density is expressed as 0 or 00000000 and white density is as 255 or 11111111. However, if the gray level image belongs to the double class, the shades of gray is represented between 0 (black) and 1 (white) [29]. In Figure 2.3, an example of a gray level image is shown.

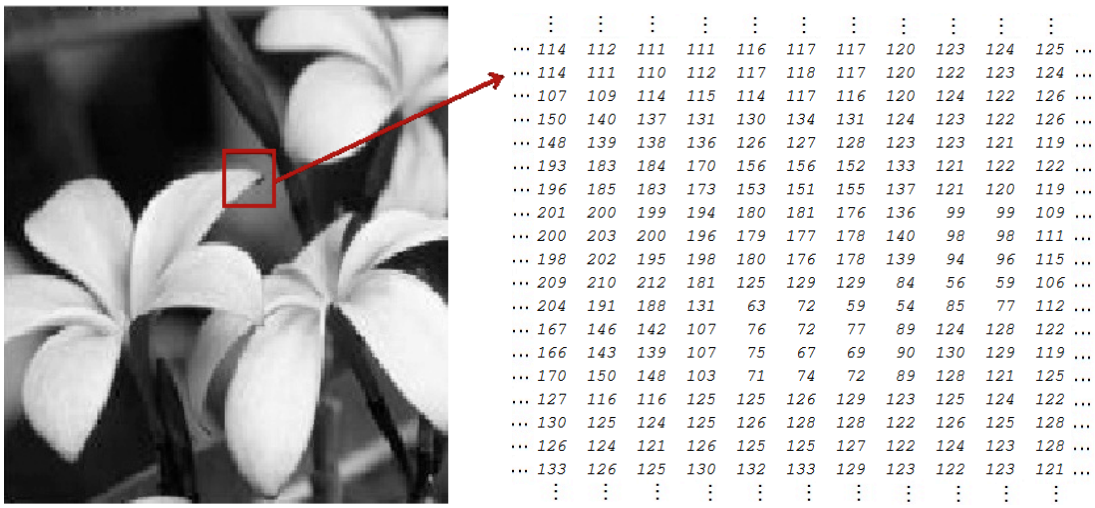

Figure 2.3 A grayscale image in the uint8 class and pixels' brightness values for a small image part

The example of a gray level image is an image belonging to uint8 class. Therefore, the brightness values of the pixels located in a small part of the image is in the range of 0-255.

A color image includes information with the higher dimensions than a gray level image. This information is red, green and blue color values used for the production of the colors in the image with different combinations [30]. Usually, a 24-bit field including 8 bits for each color component is left to determine the color of a pixel in the RGB model. Thus, each color component may take one of 256 different intensity values between 0 and 255. The colors are obtained by the use of the different concentrations of these color components. For instance, white is obtained by using three colors with 100% concentration, while black is obtained by using three colors with 0% concentration [25]. An example of the colorful image in the RGB model and its separated three color components are shown in Figure 2.4.

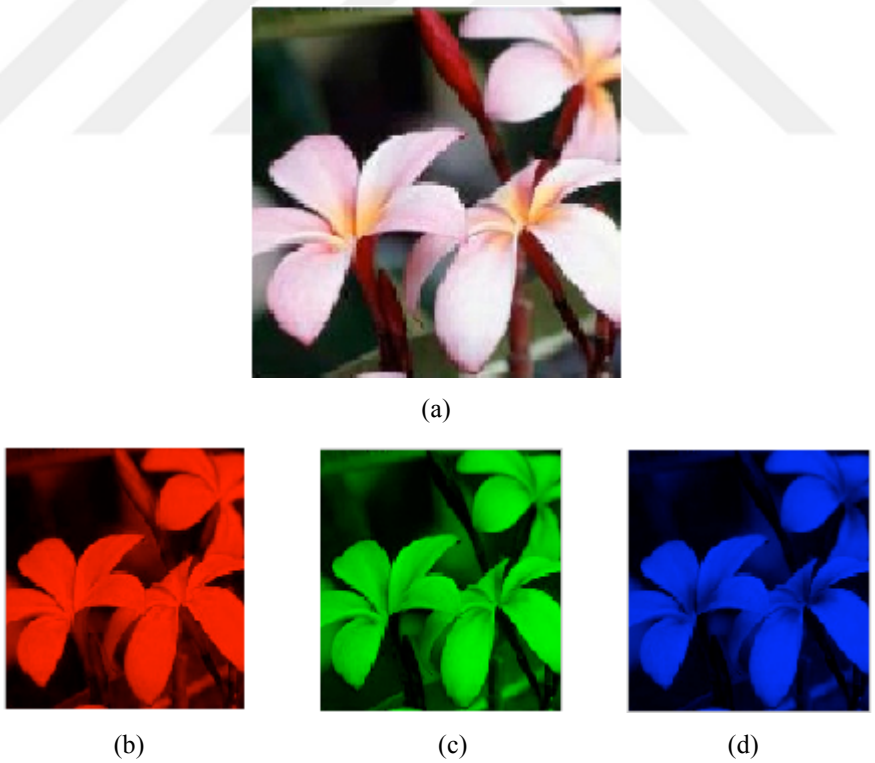

(a)

(b) (c) (d)

Figure 2.4 Flower image along with its R, G and B color components (a) RGB image, (b) R component, (c) G component and (d) B component

The color image in the RGB model consists of three matrices representing the different color components. These matrices carry red, green and blue color densities.

2.3 Image Processing

Vision is one of the most developed senses of the human beings. The view band of the electromagnetic spectrum covers a wide place from gamma waves to radio signals. Therefore, digital image processing techniques have found a wide application field.

Image processing might be described as the processing and analysis of the image with the help of the computers with the propose of extracting the information from an image or producing an alternative representation of the image. However, output is usually a new image whose quality is improved or brought to the desired shape. There are a large number of specific requirements and conditions for using image processing. Nevertheless, most of them may be classified into the following categories: (i) removing the unwanted signal components which disrupt the image and improving the visual appearance of the image for the observer, and (ii) determining and revealing the existing features and structures of the image with the conversion of the image into more pronounced and more useful form, and obtaining the needed information.

2.3.1 Filtering

Filtering in image processing is one of the basic processes used to improve the quality of the image and to ensure that it has a better view. Image filtering is often used in the applications such as noise reduction, edge detection and sharpening. Filtering concept is in the form of some frequency components removal in the frequency domain and acceptance of the rest components. While, in the spatial domain, filtering is a process that is performed on the pixel and its neighbors. Generally preferred spatial filtering techniques are median filtering, average filtering, Gaussian filtering and so on. Filtering functions are classified into two different categories; linear filters, and order-statistic filters. In the linear filtering, the

processes are carried out by convolution. For example, any pixel value in the output image is represented with the weighted sum of the values of the adjacent pixels in the input image. While a pixel value in the output image is represented by some statistics of its neighbors in the input image for order-statistics filter, such as median filter. These filters are non-linear and can not easily be applied in the frequency domain. However, the common side of the filters is that the processes are carried out in a neighborhood area including also the pixel itself. Even if the neighborhood is in different sizes, it is typically rectangular, such as 3x3, 5x5. Moreover, it need to be much smaller than the image [30]. Filtering is often performed using the convolution operation based on the neighborhood area. Formulization of this convolution process is given below.

$$s(x,y) = \sum_{m=-M/2}^{M/2} \sum_{n=-N/2}^{N/2} h(m,n) f(x-m, y-n) \qquad \textbf{(2.1)}$$

Where *h(m,n)* is a filter mask with *MxN* size. Each element in this filter mask expresses weights used usually in the linear combination. Different filter types correspond to the different filter mask. The sum of all elements in *h(m,n)* affects all density values in the output image. So that, it is sensitive to normalize, if the sum of the mask is equal to one. In the case of that *h(m,n)* includes the negative values, the sum of it is generally equal to zero. The values in the mask must be positive for the smoothing process (the low-pass filter). Otherwise, the mask contains some edges (the sharpening filter) [30].

2.3.1.1 Spatial Smoothing Filters

The smoothing filters used most commonly are averaging, Gaussian and median filters. Such filters usually have the effect of reducing the noise on the image [30].

Average Filter :

Average filter also called mean filter produces the average value of its neighbors. Filtering mask is as following (an example for 3x3 sizes):

$$h = \frac{1}{9}\begin{vmatrix} 1 & 1 & 1 \\ 1 & 1 & 1 \\ 1 & 1 & 1 \end{vmatrix} \quad \textbf{(2.2)}$$

In the practices, the mask size controls the degree of the smoothing process and the loss of details. In Figure 2.5, the filtered images of flower image in gray levels using average filter with different mask sizes is shown. It can be observed from the figure that the degree of smoothing also increases with the increase in the mask sizes of the filter.



(a) (b) (c)

Figure 2.5 Filtered images of the flower image using average filter with mask size (a) 3x3, (b) 5x5, (c) 11x11

Gaussian Filter :

Gaussian filter is an another important filter type preferred commonly. The weights in the filter mask are distributed according to Gaussian function. Mask formulation is as follows (here we assume it is isotropic):

$$h(m,n) = \frac{1}{2\pi\sigma^2} \exp\left(-0.5 * (m^2 + n^2)/\sigma^2\right) \quad \textbf{(2.3)}$$

Here, σ defines the variance and controls the degree of smoothing. Larger σ value means the realization of the smoothing process with a greater degree. For instance, a 3x3 Gaussian filter whose σ value is 1 is represented as follows:

$$h(m,n) = \begin{vmatrix} 0.60 & 0.10 & 0.60 \\ 0.10 & 0.16 & 0.10 \\ 0.60 & 0.10 & 0.60 \end{vmatrix} \quad \textbf{(2.4)}$$

In Figure 2.6, filtered images of flower image in gray level using a Gaussian filter with different variances are shown. It can be observed from the figure that the degree of smoothing also increases with the increase in the variance value of the Gaussian filter.



(a) (b) (c)

Figure 2.6 Filtered images of flower image using Gaussian filter with different variances (a) 0.01, (b) 0.5, (c) 0.99 for mask size 3x3

Median Filter :

In image processing, the median filter is a filtering technique that is widely prefered to reduce some kind of noise on the image with high performance. It often does a better job than the other filters about removing the small point noise from the image.

The median filter considers each pixel in the image and examines at its nearby neighboring pixels to decide whether it is representative of its surroundings. Then it replaces the pixels values with the sorted median value of neighboring pixel values. In Figure 2.7, this median filter process is demonsrated for an image pixel and its neighbor pixels.

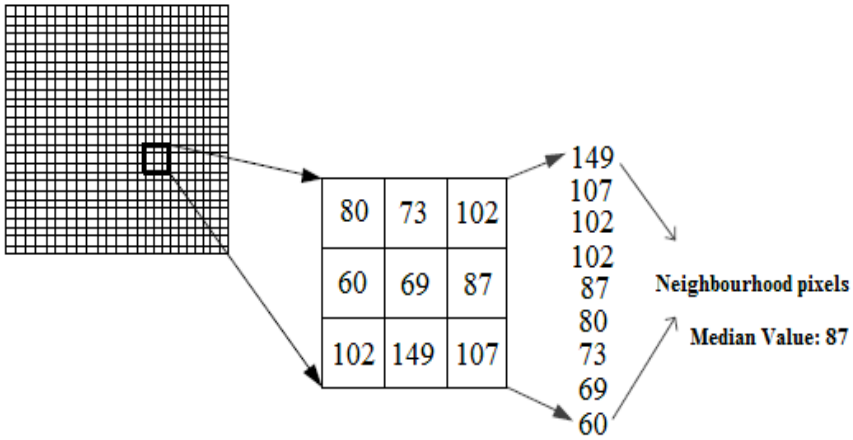

Figure 2.7 The illustration of a median value calculation

In Figure 2.8, filtered images of flower image, on which salt pepper noise was added, using median filters with masks at the different sizes are shown. It can be observed from the figure that the degree of smoothing also increases with the increase in the mask sizes of the median filter. As well, the median filter's success on protecting the edges of the objects is obviously noticed when it is compared with other filters for smoothing.



(a) (b) (c) (d)

Figure 2.8 (a) The flower image which salt and pepper noise was added on; (b) filtered image using median filter with different mask sizes 3x3, (c) 5x5 and (d) 11x11

Besides the filters mentioned above, another smoothing filters such as blurring, motion are also available. However, these filters do not have a very widespread usage. In Figure 2.9, filtered images of flower image in gray level using these filters are shown.



(a) (b)

Figure 2.9 (a) Filtered image using blurring filter with mask size 5; (b) filtered image using motion filter with two parameters of 35 and 50

2.3.1.2 Spatial Sharpening Filters

Purposes of the sharpening filters are to remove the blur from the image and to highlight important details such as edges in the image. Unlike the smoothing process uses generally the techniques based on the average of the pixels, the sharpening process is performed using spatial differentiation. Image differentiation exactly highlights edges and suppresses fields whose gray level values change slowly. Desired sharpened image is generated by adding the edge and line structures, which are obtained with image differentiation, to the original image [30]. The difference operator which is frequently applied to obtain the line structures and edges is high pass filter. The sharpening process may be expressed as follows:

$$f_{sharp}(x,y) = f(x,y) + k * g(x,y) \quad \textbf{(2.5)}$$

Here, f_{sharp} is sharpened output image of f input; k is the scaling constant controling the degree of the sharpening; g represents the image including edges and line structures extracted with high-pass filter or unsharp filter [31]. At below, filter masks are given respectively for the high-pass filter and unsharp filter.

$$H_h = \frac{1}{4}\begin{vmatrix} 0 & -1 & 0 \\ -1 & 4 & -1 \\ 0 & -1 & 0 \end{vmatrix} \quad \textbf{(2.6)}$$

$$H_s = \frac{1}{4}\begin{vmatrix} 0 & -1 & 0 \\ -1 & 8 & -1 \\ 0 & -1 & 0 \end{vmatrix} \quad \textbf{(2.7)}$$

High Pass Filter :

A high-pass filter is a kind of filter that passes high-frequency signals or elements and attenuates signals or elements with lower frequencies than the cutoff frequency. In image processing, high pass filter is the base of many sharpening methods and used to make an image appear sharper [32]. These filters extract the fine details with the high frequencies in the image. In Figure 2.10, a simple example implementation of high pass filter is given.

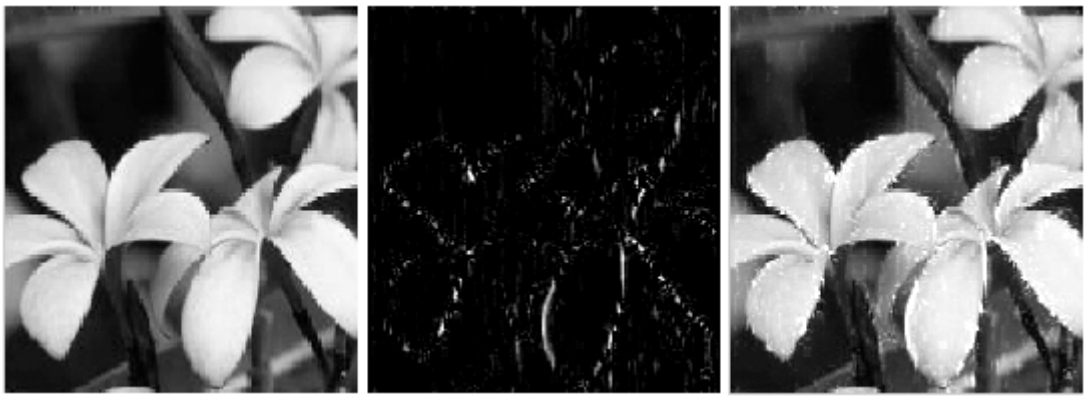

(a) (b) (c)

Figure 2.10 Sharpening process (a) the flower image; (b) extraction of the details with high frequency from the image with high pass filter; (c) sharpened image obtained with placement of the details on the image

The sharpened image can be obtained with adding the details extracted with high pass filter to original image. So that, adding the important details to the image provides higher quality, more highly contoured and understandable form of image, as seen in Figure 2.10.

Besides the high pass filter, another sharpening filter such as unsharp, prewitt and sobel filters are also available. These filters have a very widespread usage, too. In

Figure 2.11, filtered images of flower image in gray level using these filters are shown.

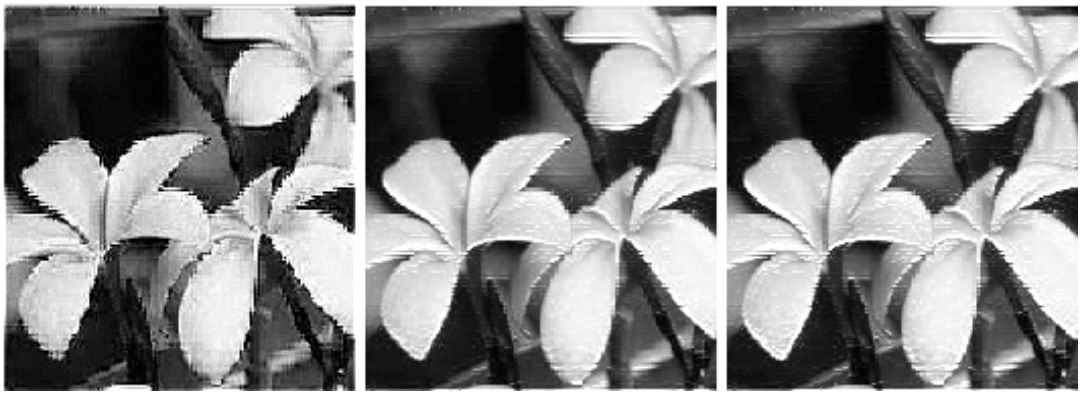

(a) (b) (c)

Figure 2.11 Filtered images using (a) unsharp filter; (b) prewitt filter; (c) sobel filter

2.3.2 Morphological Operations

Morphological image processing is a tool that is used to obtain the information about the shape and structure of an object in the image. Although morphological operators such as dilation, erosion and skeletonization can be generalized for also gray and colorful images, they are generally much more useful and meaningful processes for the analysis of binary images. Morphological operators are non-linear and used widely in the applications including filtering, edge detection, feature detection, counting objects in an image and noise reduction [33].

Basic operations of binary morphology are usually performed by a probe called as Structuring Element (SE). Structuring elements might be considered as another binary image which is quite smaller than the original image. Disk, ellipses, square and diagonal geometry can be used as SE, as well as any arbitrary shape. SE's size and shape are rather important for most applications. Structuring Element changes smaller details of the original image than SE, while not change bigger basic structures than SE [9].

2.3.2.1 Mathematical Morphology

Mathematical morphology area provides a great contribution with presenting a wide variety of operators to image processing. All of the operators are based on only several simple mathematical concepts from the set theory which is Boolean logic operations as “AND”, “OR”, “XOR” (exclusive OR) and "NOT". For example, "union" operation (AUB) is equal to "OR" operation and "intersection" operation (A∩B) is equal to "AND" operation for a binary image [33, 34]. Figure 2.12 shows a sample application of these basic operations on a binary image.

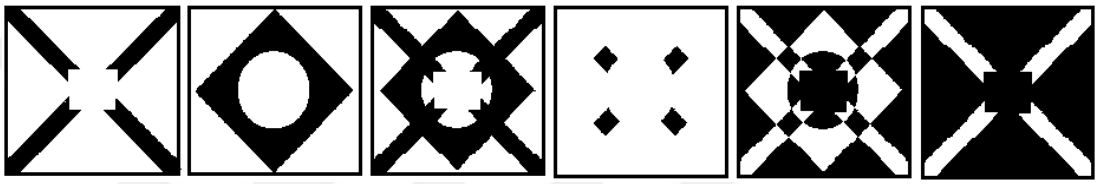

(a) (b) (c) (d) (e) (f)

Figure 2.12 Basic Boolean logical operators: (a) binary image A; (b) binary image B; (c) A AND B; (d) A OR B; (e) A XOR B; (f) NOT A

2.3.2.2 Morphological Operators

There are many morphological operators. However, the most basic two operations of them are dilation and erosion. All other morphological operations such as opening and closing are produced from different combinations of these two [33].

Dilation :

In the binary image, dilation is a process increasing the size of the front objects which are generally white pixels but the opposite is valid in some applications. In this case, SE is superposed with each pixel of the input image. So, the central of SE overlaps with the position of input pixel. If at least one pixel in SE coincides with a front pixel in the image, front pixel value is placed to the output pixel in the new image. Thus, some of the background pixels in the input image join to the front pixels in the output image. At the same time, the front pixels in the input image

remain as the front pixels also in the output image [33]. Morphological dilation causes expansion around the shape of the front pixels [9].

While "I" represents original image and "S" represents SE, dilation process can be defined as follows:

$$I \oplus S \tag{2.8}$$

In Figure 2.13, the original image is subjected to dilation operation with two different types of SE for different repetition values. In this example, SEs in the form of line and octagon were used.

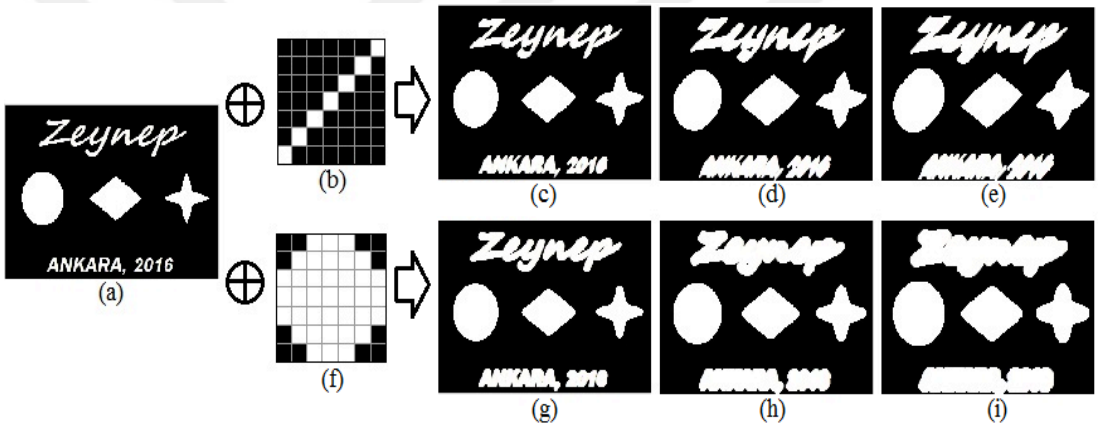

Figure 2.13 Example of morphological dilation. (a) A binary input image; (b) A line structure element with mask parameter 9 and 45; (c) Dilated image of (a) by SE (b); (d) After twice dilation by SE (b); (e) After three times dilation by SE (b); (f) An octagonal structure element with mask parameter 3; (g) Dilated image of (a) by SE (f); (h) After twice dilation by SE (f); (i) After three times dilation by (f).

Erosion :

In the binary image, conversely dilation, erosion is a process increasing the size of the background objects (and making smaller the size of the front objects). In this case, SE is superposed with each pixel of the input image. So, the central of SE overlaps with the position of input pixel. If at least one pixel in SE coincides with a background pixel in the image, background pixel value is placed to the output pixel in the new image. Thus, some of the front pixels in the input image join to the background pixels in the output image. At the same time, the background pixels in

the input image remain as the background pixels also in the output image [33]. Morphological erosion causes abrasion around the shape of the front pixels [9].

While "I" represents original image and "S" represents SE, erosion process can be defined as follows:

$$I \ominus S \tag{2.9}$$

In Figure 2.14, the original image is subjected to erosion operation with two different types of SE for different repetition values. In this example, SEs in the form of line and octagon were used.

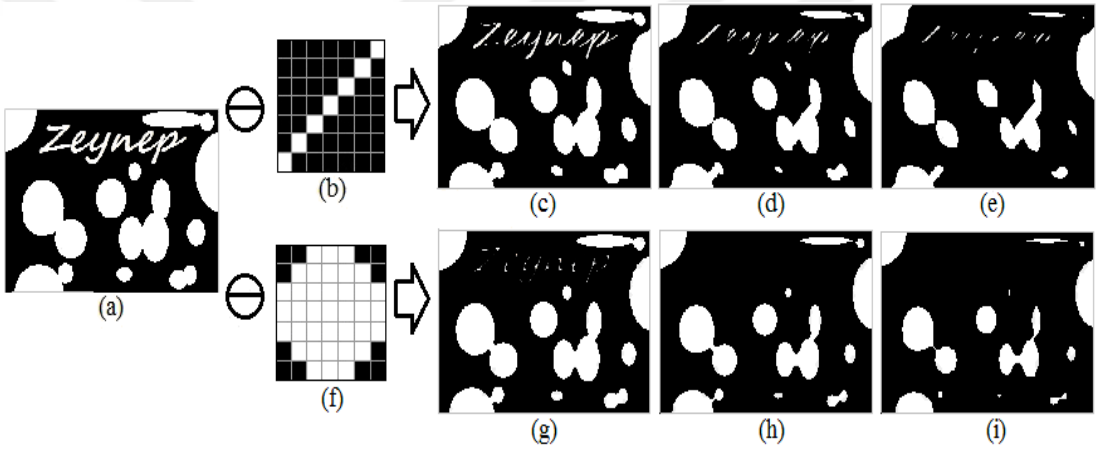

Figure 2.14 Example of morphological erosion. (a) A binary input image; (b) A line structure element with mask parameter 9 and 45; (c) Eroded image of (a) by SE (b); (d) After twice erosion by SE (b); (e) After three times erosion by SE (b); (f) An octagonal structure element with mask parameter 3; (g) Eroded image of (a) by SE (f); (h) After twice erosion by SE (f); (i) After three times erosion by (f).

Opening :

Implementing of the dilation operation after erosion operation on an image is called as morphological opening [9]. While the erosion part of this process removes some pixels from the edges of the front pixels, dilation part adds front pixels to edges. So that, foreground objects maintain the same size specifications, but their contours become more shapely. Isthmuses are broken and thin protrusions are eliminated. The effect on a binary image of the opening process depends on the structure of SE.

While this process protects the areas of front pixels whick have similar shape with SE, it tends to destroy regions which do not have the same shape [33].

While "I" represents original image and "S" represents SE, opening process can be defined as follows:

$$I \circ S = (I \ominus S) \oplus S \tag{2.10}$$

$\ominus$ and $\oplus$ indicate respectively the erosion and dilation. In Figure 2.15, a sample image is subjected to opening operation.

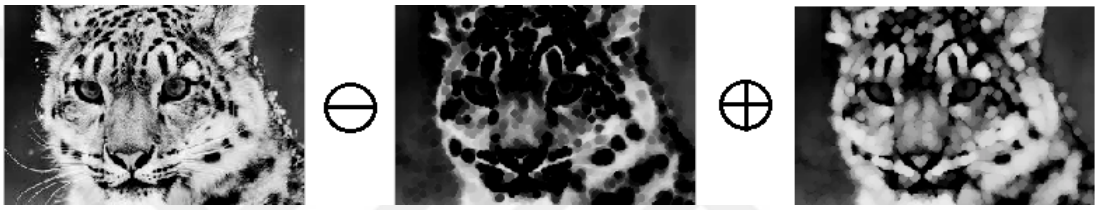

(a) (b) (c)

Figure 2.15 Opening of a gray-scale image with an 7x7 octagonal SE; (a) a gray-scale image; (b) eroded image by an octagonal SE; (c) dilated image by the same octagonal SE after erosion

Morphological opening is a process which scans the image by SE and so, eliminates hard corners and smaller objects than SE [9].

Closing :

Implementation of the erosion operation after dilation operation on an image is called as morphological closing [9]. While dilation part of this process adds front pixels to edges, the erosion part removes some pixels from the edges of the front pixels. This process smoothes the contours of the front objects. However, unlike the opening, it combines narrow fractures or gaps, and eliminates small holes [33].

While "I" represents original image and "S" represents SE, closing process can be defined as follows:

$$I \bullet S = (I \oplus S) \ominus S \tag{2.11}$$

$\oplus$ ve $\ominus$ indicate respectively the dilation and erosion. In Figure 2.16, a sample image is subjected to closing operation.



(a) (b) (c)

Figure 2.16 Closing of a gray-scale image with an 7x7 octagonal SE; (a) a gray-scale image; (b) dilated image by an octagonal SE; (c) eroded image by the same octagonal SE after dilation

Morphological closing is a process which scans the image by SE and so, fills smaller gaps and holes than SE [9].

Opening and closing operations are usually used to clean artefacts of the image prior to analysis. Selection of which processes will be used or usage order of erosion and dilation depend on the image and front objects. For example, the opening operation is used when image has noise in the foreground or long and thin features are desired to eliminate. If the possibility of the fact that first erosion operation may cut the regions is available, it is not used. The closing operation is used when a foreground region become disconnected and the connection is desired to restore. In the case that different regions are in very close locations, it is not used due to the possibility of the fact that first dilation operation may establish the connection between regions [33].

2.3.3 Segmentation

Segmentation is the separation process of an image into meaningful regions. It is generally used to distinguish desired region or object from the background [33]. At the same time, Wismüller et al. have described segmentation as the identification of significant components of the image [35]. In medical imaging, this basic analysis technique is used to delineate automatically the different components of a image; to analyse types of anatomic structures and tissues; to detect organs such as brain, heart,

liver and lungs from CT or MR images; to segment different pathological tissue such as tumor from the normal tissue [33, 36, 37].

In the segmentation analysis, the classification of foreground and background is available as the simplest implementation and a binary image is obtained as segmented image [33]. When color changes are used for image segmentation, primarily border-based approaches determining the boundary line of objects such as sobel, prewitt and roberts can be used [8, 38]. This border-based segmentation carries out the separation process with determining the edges between regions owning different properties [37]. As well as border-based approaches, segmentation techniques based on region or area are also available. They define image regions providing a certain homogeneity criterion and forming actually object with the same pixels [37, 38].

2.3.3.1 Thresholding

Thresholding connected with intensity and brightness is much simple and very strong partitioning technique despite of its simplicity, which is used to separate the objects with different brightness from darker background [33]. Thresholding process obtains binary image from gray level image containing shades of gray between white and black [39]. This method's success on the separation of the pixels at different classes and extraction of object from the background depends on the selection of the optimal threshold value (T) for the image [33, 40].

Otsu Threshold, which is one of the most commonly used types of thresholding, uses only one threshold value to obtain the binary image $g(x,y)$ from the original image $f(x,y)$ [41]. Any (x, y) point is object point if it provides the $f(x, y) \geq T$ condition, otherwise it is separated as the background [8]. In this assumption, T constant is called as *single global threshold* [38]. Thresholded $g(x, y)$ image is expressed as following [41]:

$$g(x,y) = \begin{cases} 1, & f(x,y) \geq T \\ 0, & otherwise \end{cases} \quad \textbf{(2.12)}$$

Pixels marked with *1* are white pixels belonging to object, while ones marked with *0* are black pixels belonging to background [33, 38]. An example application of Otsu Threshold segmentation is presented in Figure 2.17.



(a) (b)

Figure 2.17 Application of Otsu Threshold segmentation; (a) gray level image and (b) segmented image with the treshold value of 190

Image pixels are separated into two different classes by Otsu thresholding method. In the example given above, flowers form the first class, while others form the second class. The separation of flowers from the background and other objects in the image is provided the most successful with 190 threshold value.

CHAPTER 3

IMAGE ANALYSIS

Image analysis is the extraction of meaningful information from images. It includes all scales from simple processes like reading a barcode label to complicated tasks like the recognition of a person from his/her face [42]. Image analysis contains high level functions used for extraction of high-level information such as recognition, pattern recognition, detection of objects, tracking, classification, object counting and sizing from image or video frame.

Object counting is a very common task needed and performed in different industries. In image analysis, it is a requirement to determine how many objects is available in an image. Object counting is used to obtain the exact number of elements in the image. The result of this process function is a source of information for the quantitative analysis [22].

Conventional methods used to count objects are manual, time consuming and non-automatic forms. Continuous counting leads to eye fatigue and affects the accuracy of the results. However, even if the object counting process is performed manually, it is not simple or trivial. In fact, it might have a critical role in some applications. So that, manual methods which are time-consuming and might produce inaccurate results must be replaced with computer vision methods [43]. Automatic counting of various objects, such as cells [19], Red Blood Cells (RBCs) [20], fish [21], eggs [18] and so on, has been a subject receiving much attention in the past few years. Because of the fact that automatic counting is objective, reliable and reproducible, the comparison of the results between a great number of the images are more accurate with automatic counting program than manual counting. A user may get a different result with each measurement of manual counting, while automatic programs obtain consistently a unique value [22].

Recently, object counting has become an interesting current topic for the researchers. However, this issue can be a difficult and laborious process in the cases of objects are not able to be distinguished easily, have different sizes or are surrounded by a noisy background. To overcome these difficulties, several major counting algorithms which produce accurate results were proposed. These are hough transform, connected components and blob analysis. In addition to these counting methods, IWS method on the object counting and sizing is proposed in this thesis.

3.1 Blob Analysis

Blob analysis is a basic technique of the machine vision based on the analysis of consistent regions in the image. It has been a tool preferred frequently in the applications where the examined objects are clearly distinguishable from background. Various sets of the blob analysis methods allow the creation of special solutions for a wide range of the visual detection problem. The most important advantages of this technique are its high flexibility and excellent performance. On the other hand, its limitations are to need a transparent and clear background-foreground relationship and to have the pixel sensitivity [44].

The goal of the blob extraction is to get blobs (objects) in a binary image isolated. A blob includes a group of the connected pixels. Whether two pixels are connected, which pixels are neighbour or which ones are not defined by the connectivity parameter [44]. The title of this subject covers firstly the extraction of the blobs, then improving with removal of the various kinds of the noise, and finally the classification of the type of every blob and the analysis of binary images with decomposition of a region to specific blobs if this region represents objects more than one. For the realization of the counting process, each blob is assigned to value representing them and the number of blobs is determined with counting the levels [44, 45]. In Figure 3.1, a sample application of the object counting performed using blob analysis is shown.

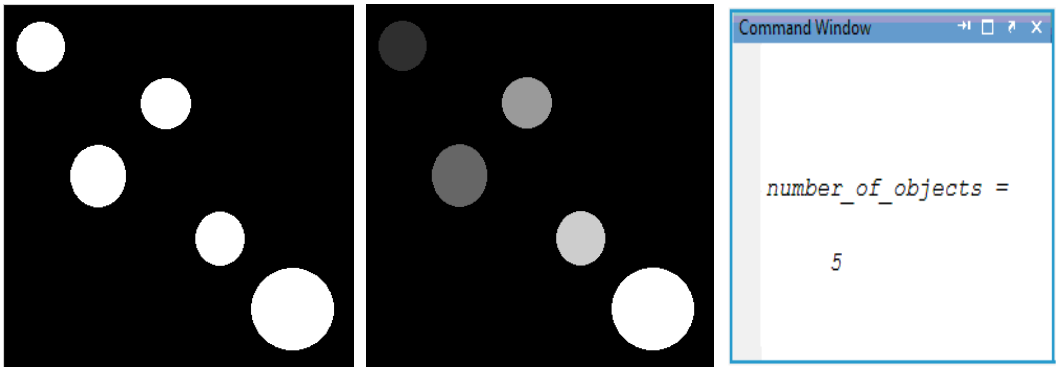

(a) (b) (c)

Figure 3.1 An example application of object counting using Blob analysis method (a) a binary digital image as input; (b) the output image whose objects are labeled to a unique level; (c) the algorithm's result giving the counted number of objects

In a study on this subject, an automated cell counting method based on blob analysis in the microscopic images were introduced by Xiaomin Guo and Feihong Yu [19]. In that study, blob analysis was used to detect blobs in the image and to determine the selection parameters of these blobs. The results about calculated total number of the obtained cells showed that maximum relative error is 1.33%, minimum relative error is 0% and average relative error is 0.46%. In a similar study performed by Fabic et al., an effective method which detects, counts and classifies the fishes on the underwater video frames using blob analysis and shape analysis was presented [21]. In the study, blob counting process was one of the four major steps of the proposed system and the number of examined fish objects was determined by this process. Blob detector was based on Laplacian of Gaussian (LoG). In the results, it was observed that tolerance was less than 10%.

3.2 Hough Transform

Hough transform is one of the classic computer vision techniques that is based on almost 50 years back [46]. Initially, it has been proposed as a method for the determination of the line structures in the edge maps. However, then it has also been extended to detect low-parametric objects like the circle [47]. In the recent years, Hough-based methods have been adapted successfully to the problems on the part-based category-level object detection [48-54].

Disadvantage of Hough transform in the standard applications is the need of a large storage space and high level computing [55]. In addition, the shape characteristics of the object desired to be detected are important requirements for the algorithm. The requirement of such prior knowledge is among the limitations of the algorithm. In Figure 3.2, an example application of the object counting performed using circular Hough transform is shown.

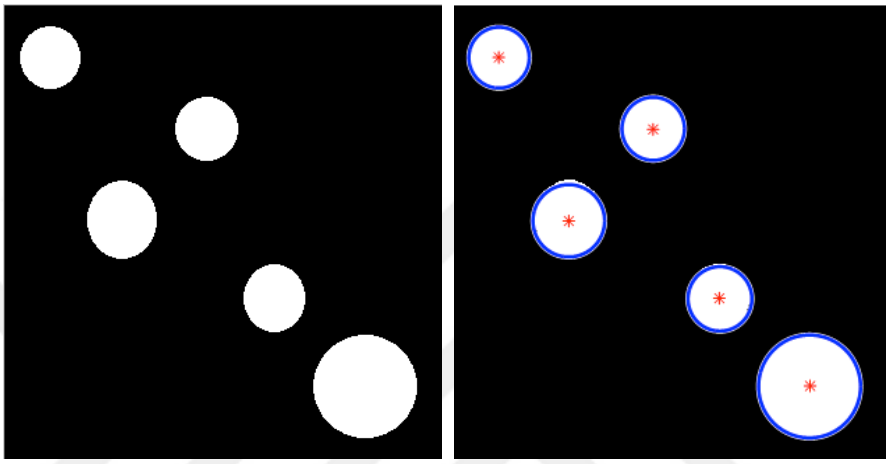

(a) (b)

Figure 3.2 An example application of object counting using circular Hough Transform (a) a binary digital image as input; (b) the output image whose objects are bounded with blue circles and their centers are marked with red plus sign

Method presented by Venkatalakshmi and Thilagavathi may be given as the example of the studies on this subject in the literature [20]. Hough transform was used in the method which they developed for automatic red blood cells (RBCs) counting. Circular Hough transform was applied to extract RBCs in the feature extraction and count step of the RBCs' prediction algorithm. Similarly with this study, circular Hough transform method was also used by Reddy to form an effective and efficient computer vision system that performs the automatic counting of RBCs and white blood cells (WBCs) [56]. In addition to these literatures, an algorithm for the count of red blood cells in urine sediment was proposed by Watchara et al. using again Hough transform [57]. Circular Hough transform was used in the counting process of the blood cells which is the last step of the algorithm. It was shown with the

experimental results that the average error percentages of the detection of RBCs and WBCs were obtained respectively 5.28 and 8.35.

3.3 Connected Component Analysis

Connected component labeling is an algorithmic implementation of the graph theory whose connected compounds' sub clusters are labeled uniquely. This method should not be confused with the segmentation process. Connected component labeling is used in computer vision to detect connected regions in the binary digital images [58].

An algorithm of connected component labeling finds all points in the same component and assigns to a unique single level. Labeling may be carried out with 4 or 8 connectivity parameters. 4 parameter specifies 4 connected objects, while 8 parameter specifies 8 connected objects where diagonal connections are possible [59]. In Figure 3.3, an example application of object counting performed using Connected Component analysis.

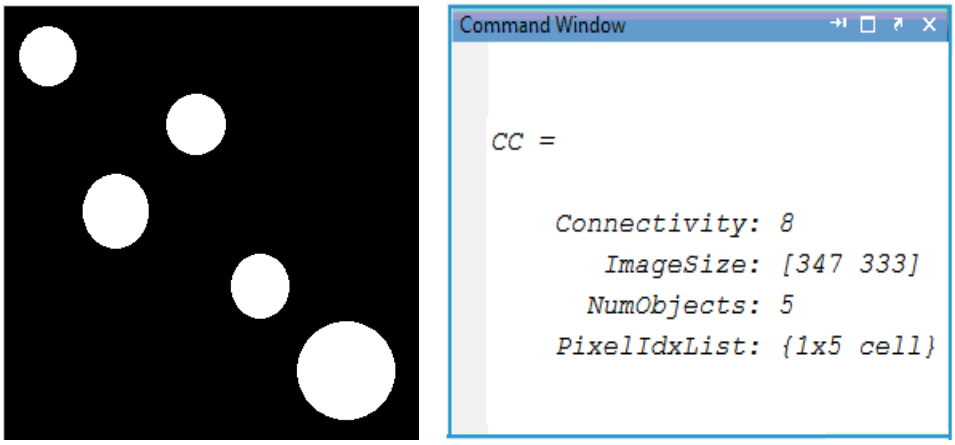

(a) (b)

Figure 3.3 An example application of object counting using Connected Component method (a) a binary digital image as input; (b) the algorithm's result giving the counted number of objects depend on the connectivity parameter

In a study in which this method was used, a system for the identification and classification of the objects whose number is more than one was produced by

Dimitriou et al. [60]. In that study, the Connected Component method was applied on the image in which objects' edges were extracted. As a result of this process, each object was detected, and also some useful information such as extreme points and bounding box of each component was obtained. In another study on this subject, two-level tagging algorithm based on Connected Component analysis is defined for the object tracking by Halgaonkar [61]. In addition to these studies, Connected Component labeling was also used in order to determine all objects in the image in another study [59]. All connected components were found with this labeling algorithm and all points in the same component were assigned to a unique single level for counting the logs in a timber truck. The results of that study showed that segmentation and average counting of the logs were performed with about 97% accuracy.

In the literature, another different techniques from mentioned counting methods are also available. For example, a method for counting the microorganisms was presented by Barbedo [62]. In that study, a series of morphological operations was used to obtain display which would provide easily the isolation and counting of the desired objects. In another study, image analysis was used by Ramin et al. to obtain the number of the cells in the immunocytochemical images [63]. Cell counting process was made with tracing the boundaries. In another study, two methods were presented for counting the number of mosquito eggs by Mello et al. [18]. Those methods were based on different color models.

3.4 Image Weight Signal (IWS)

Although difficulties on the object detection and counting were almost overcome by the methods proposed in the literature, there is not enough work about object sizing. Therefore object sizing topic stil involves many challenges needed to be solved. In the object counting algorithms, only object detection is sufficient. However, object sizing includes challenge on the separation of an object from other objects to evaluate the size, as well as object detection. In addition, that object sizing process is repeated for each object detected in the image brings the issues of the time, memory

and processing load. Nevertheless, lack in the object sizing topic is felt clearly in vital fields such as biomedical area despite of these difficulties needed to be overcome. In the presented study, Image Weight Signal (IWS) is proposed in order to overcome the difficulties of the sizing issue, in addition to object counting.

IWS is a signal obtained by scanning of a black and white image and calculating the intensity at each scanning window. Although IWS is a one-dimensional information, it carries some spatial information of the image. It is possible to obtain the number of the objects and size parameters of the objects from this signal carrying spatial information. Two different scanning methods can be used to obtain the IWS. Selection of vertical or horizontal scanning depends on the location of the objects in the image. In the same way, if objects are aligned on the horizontal plane, the horizontal scanning is used. If objects are aligned on the vertical plane, the vertical scanning is used. If objects are aligned on the diagonal plane, both scanning methods can be used. The selection of scanning method for obtaining IWS affects the accuracy of the results produced by algorithm. In Figure 3.4, sample images whose objects are aligned on different planes and their appropriate scanning methods are given.

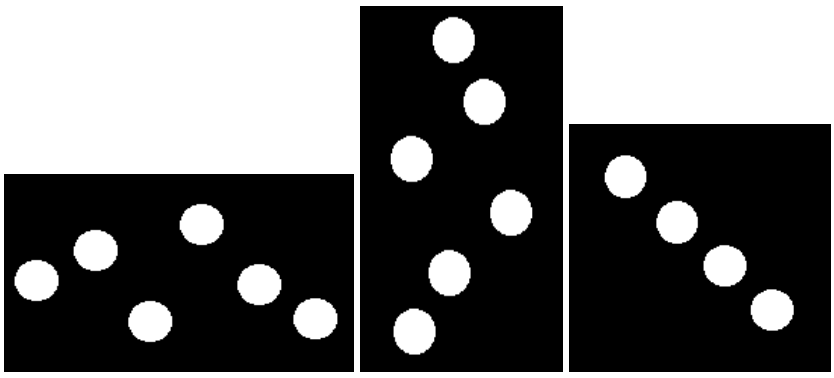

Figure 3.4 The example images whose objects are alined on (a) horizontal plane for IWS with horizontal scanning, (b) vertical plane for IWS with vertical scanning, and (c) diagonal plane for IWS with both scanning types

Mathematical formulation used to obtain IWS from *im* which is a binary image is given in equation 3.1. Equation 3.1a represents IWS obtained by vertical scanning, and equation 3.1b represents IWS obtained by horizontal scanning.

$$\text{signal_function}(k) = \frac{\sum_{i=s}^{a}\sum_{j=1}^{b} im(i,j)}{(a-s+1)*b} \tag{3.1a}$$

$$\text{signal_function}(k) = \frac{\sum_{i=1}^{a}\sum_{j=s}^{b} im(i,j)}{(b-s+1)*a} \tag{3.1b}$$

Here, *a* and *b* represent respectively row and column numbers of the image *im*. *k* is an array with the same length of IWS which will be produced. The length of this array depends on the number *n* of the scanning windows.

k=1,2,3,4,……,n;

$$n = \begin{cases} a/sensitive, & mod(a,sensitive) = 0 \\ floor(a/sensitive) + 1, & mod(a,sensitive) \neq 0 \end{cases} \tag{3.2a}$$

$$n = \begin{cases} b/sensitive, & mod(b,sensitive) = 0 \\ floor(b/sensitive) + 1, & mod(b,sensitive) \neq 0 \end{cases} \tag{3.2b}$$

Equation 3.2a is used for vertical scanning, while equation 3.2b is used for horizontal scanning. *sensitive* value seen in the equations is a parameter providing the balance between accuracy and speed of the algorithm. *s* parameter array whose formula is given in equation 3.3 depends on *k* array and *sensitive* value. This parameter provides the movement of the scanning window.

$$s = 1 + ((k-1) * sensitive) \tag{3.3}$$

Matlab code of the mathematical formulation explained above for obtaining IWS is given in Algorithm 1.

Algorithm 1 :

```
1  define variable a;                % the row number of the 'im' image
2  define variable b;                % the column number of the 'im' image
3  define variable sensitive;        % method parameter
4  define variable n;                % the length parameter of the weight signal
5  define variable k;                % method parameter
6  sensitive = 3;
7  k = 0;
8  if mod(a,sensitive) ≠ 0, start
9     n = floor(a/sensitive)+1;
10 else n = a/sensitive, start
11 end
12 define array amount(n); % the total pixel number of the calculation windows
13 define array signal_function(n);    % the image weight signal
14 while provide the condition (k<n), start the loop
15 k = k+1;
16 s = 1+((k-1)*sensitive);
17 amount(k) = (a-s+1)*b;                % if the scanning type is vertical
                    % amount(k) = a*(b-s+1), if the scanning type is horizontal
18 signal_function(k) = sum(sum(im(s:a,1:b)))./amount(k);
                                        % if the scanning type is vertical
                    % signal_function(k) = sum(sum(im(1:a,s:b)))./amount(k),
                                        % if the scanning type is horizontal
19 end the loop (k = n);
20 plot(signal_function);
```

An example application of this algorithm and IWS function obtained as the result of the algorithm is presented in Figure 3.5.

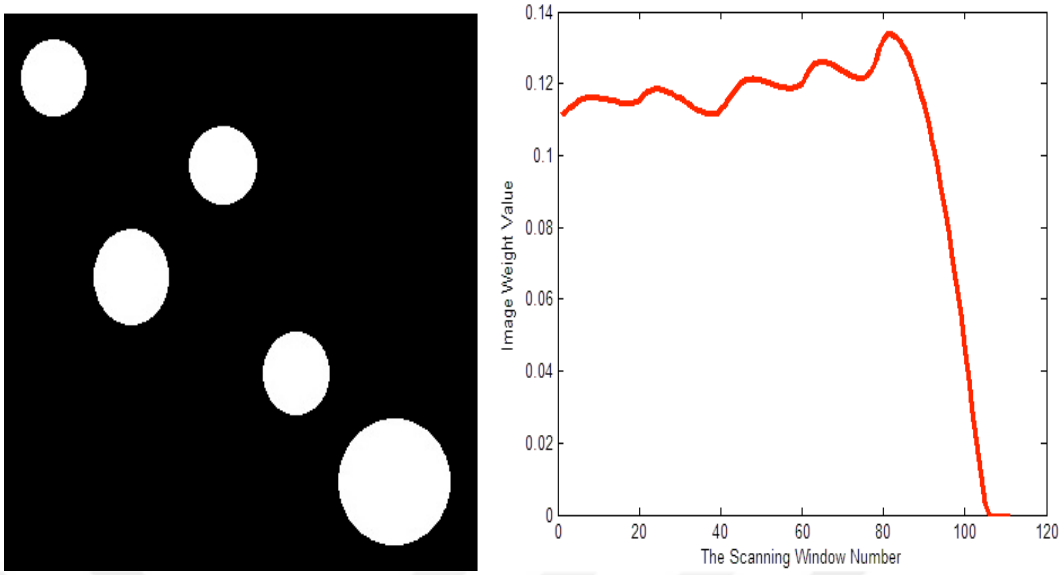

(a) (b)

Figure 3.5 An application of Algorithm 1 on (a) black-white *im* image and (b) obtained IWS function graph with vertical scanning as the result of the algorithm

Detection of the objects in the input *im* image is performed with obtaining IWS function by Algorithm 1. Decomposition process of these detected objects is performed on the derivative function of the IWS. This process is a requirement to examine sizes of the objects. In equation 3.4, the derivative function used to obtain the decomposition points of the objects is given.

$$\text{derivative_signal} = \frac{\text{d(signal_function)}}{\text{dt}} \tag{3.4}$$

Here, *t* is equal to *amount* array which includes the total number of the pixels within each scanning window. It was determined that the decomposition points of the target object regions are local minimum points in the derivative function. Equations 3.5 and 3.6 given below are used to determine these local minimum points.

$$\text{decreased_regions}(x) =$$

$$\begin{cases} \text{derivative_signal}(x+1), & \text{derivative_signal}(x+1) < \text{derivative_signal}(x) \\ 0, & \text{derivative_signal}(x+1) \geq \text{derivative_signal}(x) \end{cases} \tag{3.5}$$

Here, *x=1,2,3,4,……..,l* is an array and *l* is the length parameter of the derivative function. In this equation, decreasing regions in the derivative function are extracted for the detection of the local minimum points and recorded into *decreased_sections* array, other regions are also set to zero. At the same time, *x* values of the decreasing regions are also saved as *decreased_sections_X* array.

$$\text{decreased_regions_X}(x) = \begin{cases} x+1, & \text{derivative_signal}(x+1) < \text{derivative_signal}(x) \\ 0, & \text{derivative_signal}(x+1) \geq \text{derivative_signal}(x) \end{cases} \quad \textbf{(3.6)}$$

Matlab code which performs the detection and recording of decreasing regions in the derivative function and *x* values of these regions is given in Algorithm 2.

Algorithm 2 :

```
1  define variable t;        % the length parameter of the derivative_signal function
2  define array decreased_ sections (t-1);
3  define array decreased_ sections_X(t-1);
4  derivative_signal = diff(signal_function)./diff(amount);
5  start the loop (for from x = 1 to x = t-1)
6       if derivative_signal(x+1) < derivative_signal(x), start
7            decreased_ sections(x) = derivative_signal(x);
8            decreased_ sections(x+1) = derivative_signal(x+1);
9            decreased_ sections _X(x+1) = x+1;
10      else derivative_signal(x+1) ≥ derivative_signal(x), start
11           decreased_ sections(x+1) = 0;
12           decreased_ sections_X(x+1) = 0;
13       end;
14 end the loop (x = t-1);
15 figure, plot(turev,'b'), hold on
16 plot(decreased_region,'r')
```

A sample application of this algorithm was performed as the next stage after Algorithm 1. The derivative function of the obtained IWS and *decreased_sections* array including decreasing regions is presented in Figure 3.6.

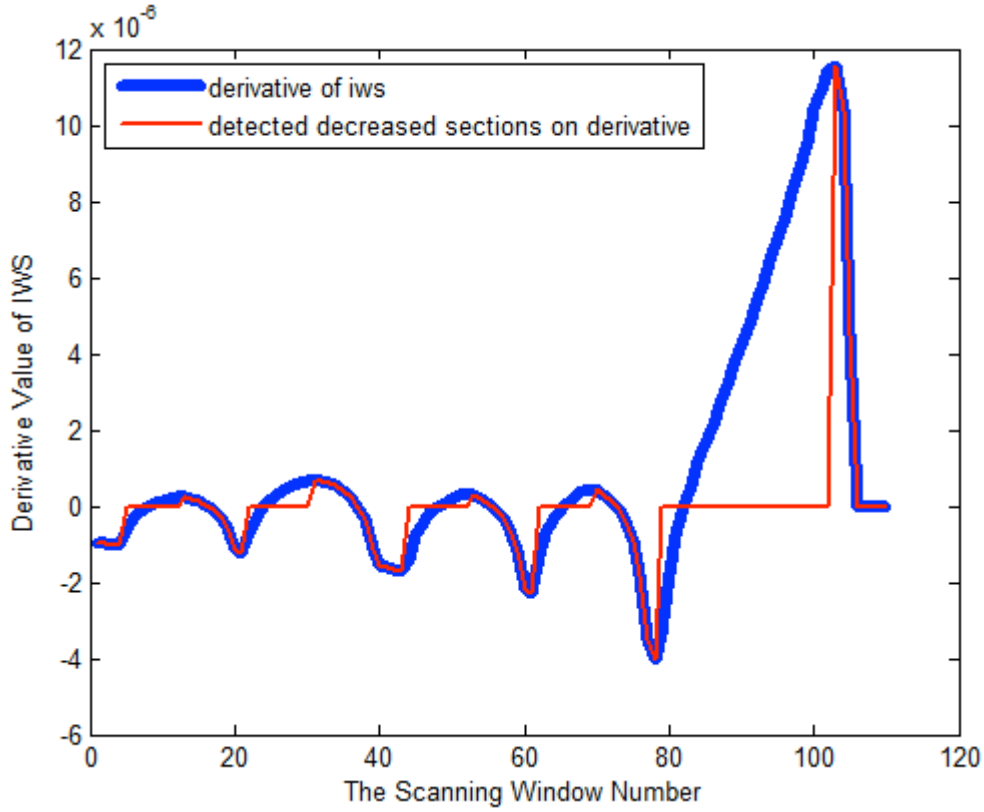

Figure 3.6 Derivative function graph of IWS and detected decreased sections on derivative function as a result of Algorithm 2

To find the minimum points of the decreasing sections in the derivative function, *x* values of each decreasing region are reformed as the column of a matrix. This process is done on the *decreased_ sections_X* array and at the end of the process, a region matrix whose each column represents a decreasing region is obtained. Maximum *x* values in the columns are *x* values of the minimum points of the decreasing sections locally separated in the derivative function. The Matlab code of the separation of the decreasing sections and process for obtaining the local minimum points in the derivative function is presented in Algorithm 3.

Algorithm 3 :

```
1  define variable l;                    % the row index of the region matris
2  define variable region_ index;        % the column index of the region matris
3  define variable w;                    % the length of the decreased_ sections_X array
4  l = 1;
5  region_index = 1;
6  w = length(decreased_ sections_X);
% obtaining step of the region_matris
7  start the loop (for from x = 2 to x = w);
8     if decreased_ sections_X(x) ≠ 0, start
9        region_matris(l,region_ index) = decreased_ sections_X(x);
10       l = l+1;
11    else decreased_ sections_X(x) = 0 and decreased_ sections_X(x-1)≠0, start
12       region_ index = region_ index+1;
13       l  = 1;
14    end;
15 end the loop (x = w);
% determination step of the local minimum points from the obtained region_matris
16 [nn mm] = size(region_matris);
17 region_matris (:,1:mm-1)     % the last column does not represent any region,
                                % so no process related with this column is done
18 local_minimum_points = max(region_matris(:,1:mm-1) )
19 region_number = length(local_minimum_points);
% marking step of the minimum points on signal_function
20 start the loop (for from x = 1 to x = region_number);
21       hold on,
22       y = [-6 :0.01:4 ]*10^-6;
23       plot(local_minimum_points(x),y,'k')
24 end the loop (x = region_number);
25 hold off
```

A sample application of this algorithm was performed as the next stage after Algorithm 2. Matlab output of matrix obtained by the separation of the decreasing

sections and the local minimum points of each region is given in Figure 3.7. Obtained local minimum points are also demonstrated graphically on the derivative function in Figure 3.8.

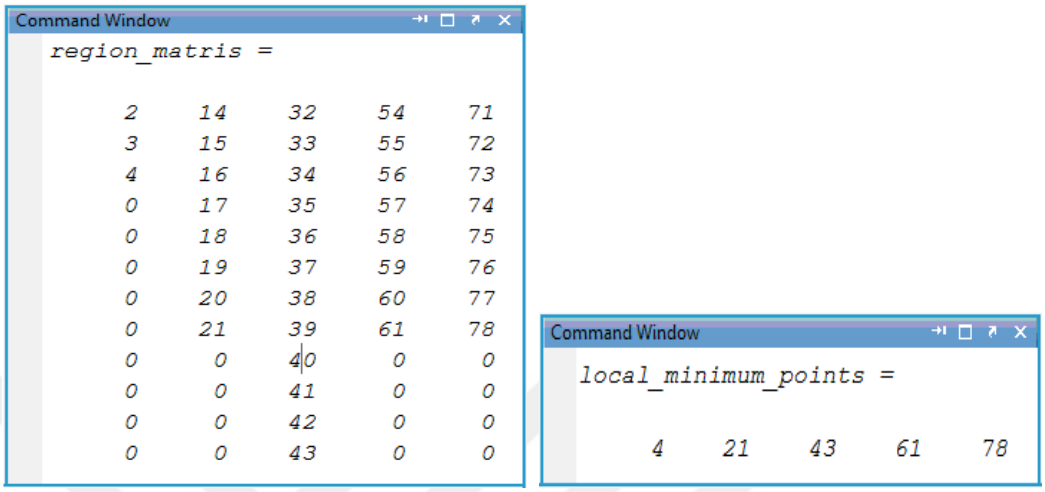

(a) (b)

Figure 3.7 As results of Algorithm 3, (a) obtained region matrix with decomposition decreased sections and (b) local minimum points of decomposed regions

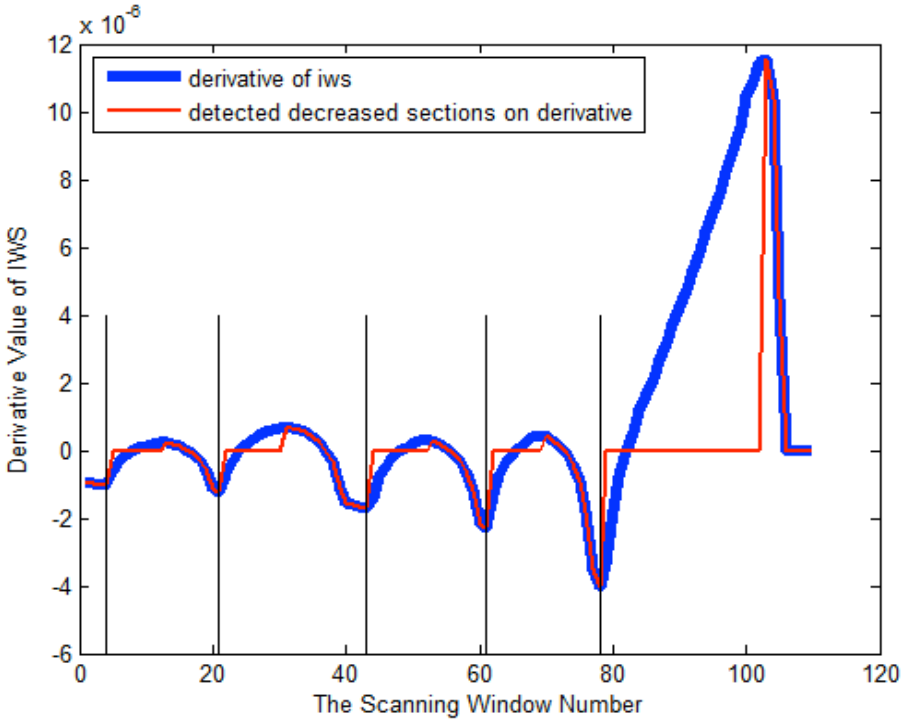

Figure 3.8 Display graph of local minimum points representing the objects on the derivative function's decreased sections

Detected minimum points in the derivative function represent objects in the image. Matlab code that performs the display of the local minimum points on the IWS is given in Algorithm 4.

Algorithm 4 :

```
1 t = 1: k                                  % the length of the weight signal
2 plot(t,signal_function,'r');
3 title('Image Weight Signal');
4 start the loop (for from x = 1 to x = region_number);
5       hold on,
6       plot(local_minimum_points(x), signal_function, 'p');
7 end the loop (x = region_number);
```

A sample application of this algorithm was performed as the next stage after Algorithm 3. Consequently, overlapped the local minimum points with the IWS are shown in the graph given in Figure 3.9.

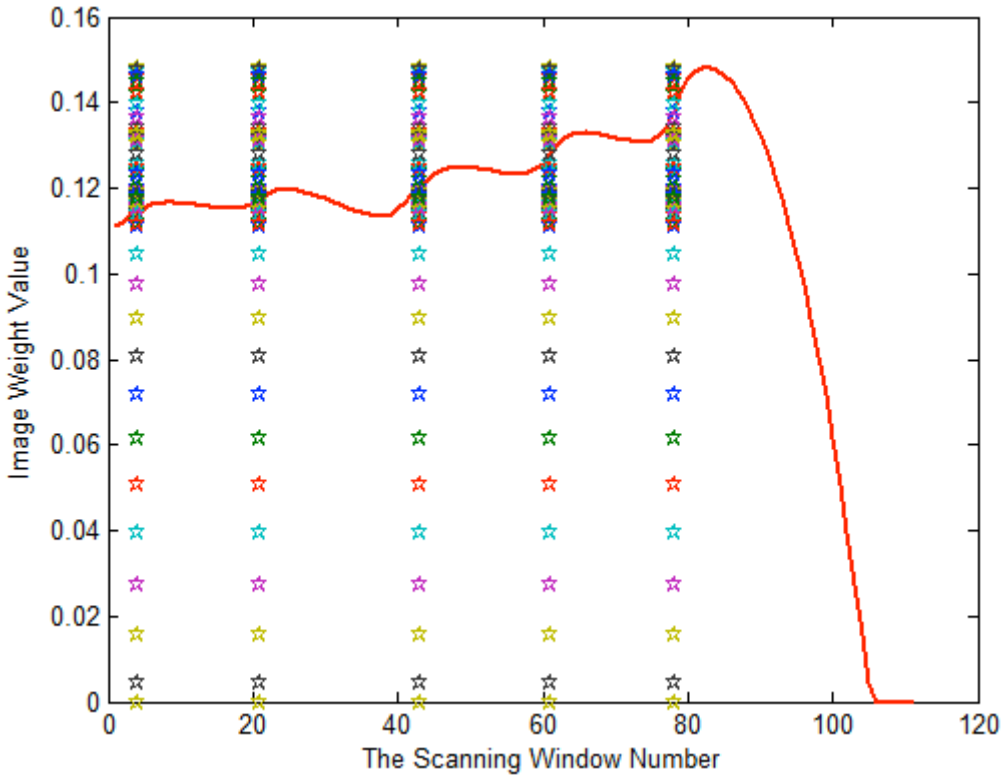

Figure 3.9 Superposition graph of the local minimum points on the IWS with vertical scanning

After the local minimum points representing the objects in the derivative function are marked on the IWS, the calculation of the area parameters of the objects can be performed. The Matlab code for the calculation of the object sizing process is given in Algorithm 5.

Algorithm 5 :

```
8  define variable a;                          % the row number of the 'im' image
9  define variable b;                          % the column number of the 'im' image
10 define variable total_pixel_number; % the pixel number of the 'im' image
11 define variable FOV;                        % Field of View
12 define array region_areas_pixel(region_number);
13 define array region_areas_cm2(region_number);
14 FOV = 8.8*9.1;                              % width and height values in cm of image
15 start the loop (for from x =1 to x = region_number);
16          region_areas_pixel(x) = amount(local_minimum_points(x))*…
17          …signal_function(local_minimum_points(x));
18 end the loop (x = region_number);
19 total_pixel_number = a*b;
20 start the loop (for from x = 1 to x = region_number);
21       if x = region_number, start
22         region_areas_cm2(x) = …
           … (FOV/total_pixel_number)*fix(region_areas_pixel(x));
23       else, start
24       region_areas_pixel(x) = region_areas_pixel(x)-region_areas_pixel(x+1);
25       region_areas_cm2(x) = (FOV/ total_pixel_number)*…
         …fix(region_areas_pixel(x));
26        end;
27 end the loop (x = region_number);
28 region_areas_pixel                  % regions' calculated areas depend on pixel
29 region_areas_cm2                    % regions' calculated areas
```

A sample application of this algorithm was performed as the next stage after Algorithm 4. The calculated size information of the objects with this code which is the last step for object counting and sizing is given as Matlab output in Figure 3.10.

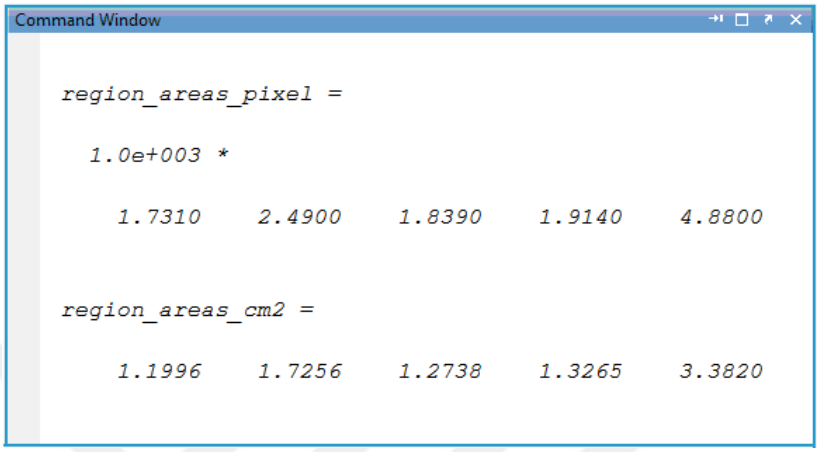

Figure 3.10 Calculated area information of the objects

IWS method developed in this study presents solution to some of the difficulties about object sizing as well as performing objects counting process.

Compared with other object counting methods in the literature, the advantages of IWS method are:

1. Generating also area information of the detected objects as a result, as well as the number of the objects. In Figure 3.11, an application of the IWS is presented.

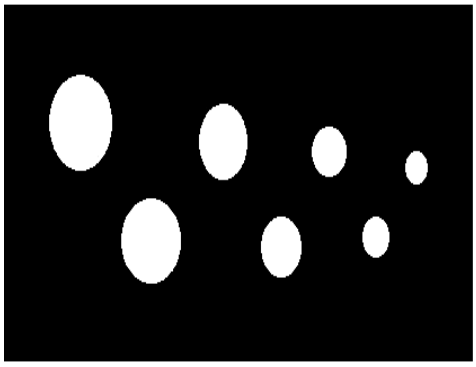

(a)

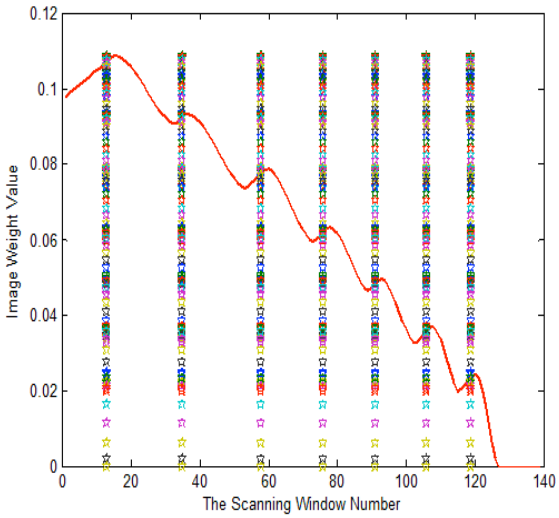

(b)

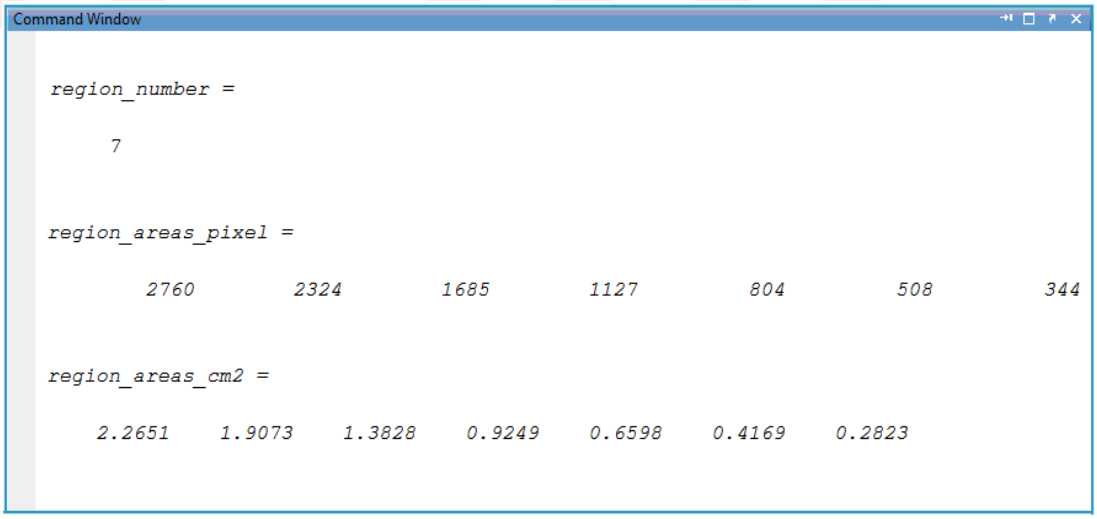

(c)

Figure 3.11 An application of the IWS on (a) the black-white image; and as a result, obtained (b) superposition graph of the local minimum points representing objects on the IWS and (c) calculated area information of the objects

2. Performing counting and sizing processes on the 1-dimensional signal which is IWS obtained from the image, not on the 2-dimensional image. It means less complex process, less processing load, less memory, less time and more processing speed on the sequence data such as CT scanning. In Figure 3.12, an application of the IWS and blob analysis on an array of images whose sizes are increasing gradually and the time comparison graph of the both techniques are presented.

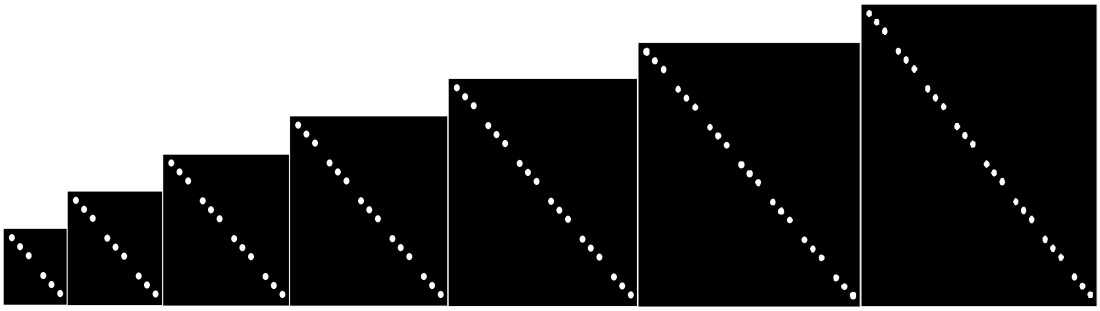

(a)

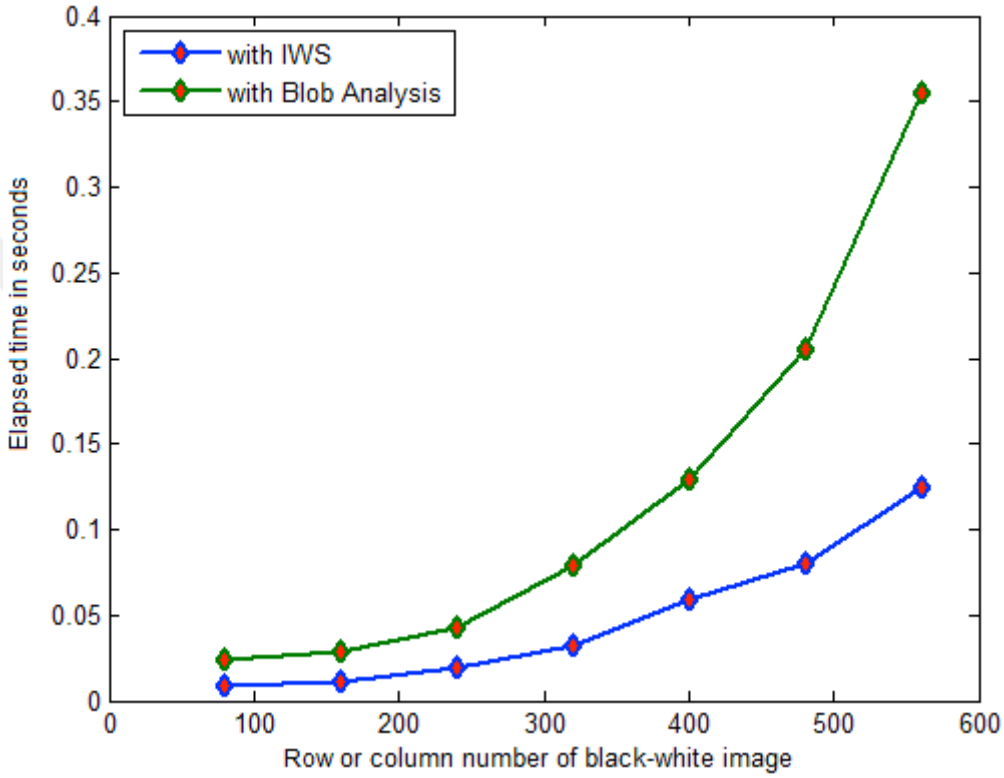

(b)

Figure 3.12 An application of IWS and Blob analysis on (a) the array of images whose sizes are increasing at each step and (b) the time comparison graph of both counting and sizing techniques on the image array

In this application, an additional algorithm which calculates separately the number of pixels for each level was added to the blob analysis which is an object counting algorithm. Thus, it could carry out also the object sizing process for comparison. The time graph produced as a result shows that the developed technique produces results fairly fast, while other technique has a sharp slowdown to produce result with increasing in the image size.

Compared with other object counting methods in the literature, the disadvantages of IWS method are:

1. Not working on the images containing many objects such as cell, rice, log. In Figure 3.13, an application of the IWS is presented.

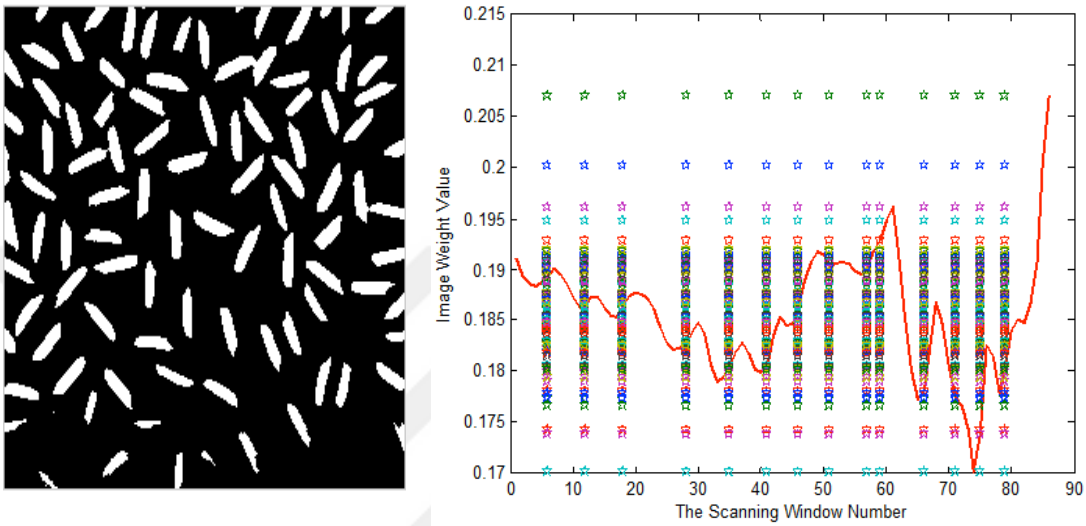

(a) (b)

Figure 3.13 An application of the IWS on (a) the black-white rice image; and as a result, (b) obtained superposition graph of the local minimum points representing objects on the IWS

This application shows that IWS method can not produce accurate results in the images containing many objects.

2. The requirement of the fact that objects must be in a specific order. The location of the objects in the image influences the accuracy of the results.

CHAPTER 4

COMPUTED TOMOGRAPHY IMAGING TECHNIQUE IN BIOMEDICAL

Today, biomedical concept consists of mechanical, electronical devices and systems which are the greatest helpers of the medical science in the diagnosis and treatment services. In the health field, importance of particularly fast, accurate and user-friendly biomedical imaging systems is increasing day by day as well as the biomedical devices. The invention of X-rays by Wilhelm Conrad Röntgen toward the late of 1800's is the discovery that forms the basis of the present medical imaging methods and causes starting of a new age in the medical science. This innovation has increased the interest on the imaging subject with its very quick spreading, and so the studies on this subject have being increased day by day [8]. Over the past century, Röntgen's scientific breakthrough has been combined with today's digital image and computer technology, so that new imaging techniques have been developed. Imaging techniques which have been able to be applied so far are divided into five main groups including X-ray, Computed Tomography (CT), Magnetic Resonance Imaging (MRI), ultrasound and radionuclide imaging. Each of these methods has different physical working principles. Therefore, the type of energy used to obtain the image and the image receptor systems are different in all methods [64]. Methods use one of three types which are electromagnetic, particle and acoustic radiation as energy form for imaging. Information about the internal structure can be obtained with getting the change in time and/or space of radiation field, which passes from the biological tissue and structure, and converting it to image [65]. Computed Tomography is among the most commonly used methods to obtain information about internal structure of the body.

4.1 Computed Tomography (CT)

Tomography is a radiological diagnostic technique which allows selectively the visualization of anatomical structures or lesions in the desired depth [66]. The basic

principle of the tomographic systems is based on the object's examination as the cross sectional. Computed Tomography device is the only system which is capable of forming the images belonging to the inner depths of the body as 3-10 mm slices with X-rays. This device uses a similar type of X-ray tubes contained in conventional X-ray devices as source. The basic of the system's imaging technique is that cross sectional radiographs are obtained with source and detector which are in opposite directions during the scanning. The discovery of CT device after conventional X-ray devices has created a huge revolution in radiology and modern medicine, and it has made human beings stronger against the cancer [8, 67].

4.2 The Development of CT Devices

CT technology which opened a new age in radiology was theorized by Cormak in 1963. The first successful clinical application was carried out by Godfrey Hounsfield in 1967, its usage in the hospital environment started in 1971. The first CT unit was established in 1973 in the USA, while the first use in our country was performed in 1976 at Hacettepe University in Ankara. In the first CT machines, data which was necessary for the creation of a single slice could be collected hardly in a long time like 5 minutes. CT applications were only used early in the brain investigation due to the length of time. This reason has delayed usage of Computed Tomography also in application field such as the thorax, abdomen [68].

4.3 The Principle of CT Device

Computed Tomography is a radiological diagnostic method used for creating cross sectional images of the examined part of the body. The basis of CT is based on a similar structure with X-ray tube technology used X-ray devices. However, unlike the other X-ray devices, tubes in this device are not constant and they are attached on the 'gantry' (the aperture of the device) which returns continuously. Thus, X-ray source performs a rotational movement of 360 ° around the patient examined. Meanwhile, the detectors which are set along 'gantry' absorb X-ray beams which pass from the patient and carry the image information [8, 67]. X-rays, which fall on the

detector after passing from the patient, cause ionization in the detector material. Electric charge which occurs as result from ionization give an analog output in direct proportion to X-ray energy and flux in the output of detector circuit, because detectors are similar to parallel plate electrodes or they are p-n junction type transistors. Analog signals obtained from the detectors during the rotation of the X-ray tube are projection information from every angle. This analog projection information collected from every angle is converted into digital data with an analog-to-digital converter (ADC) and CT images are created with processing of this digital image information on the computers connected to the CT machine. Cross sectional images are obtained with reflection of the information coming from each projection to an image matrix with 512 x 512 or 1024 x 1024 sizes which is dedicated for a slice in the memory of the computer. This process is repeated for analog information from each cross section. As a result, consecutive cross sectional images of tissues are formed [67, 69]. The basic elements and operation of the CT system is shown in Figure 4.1.

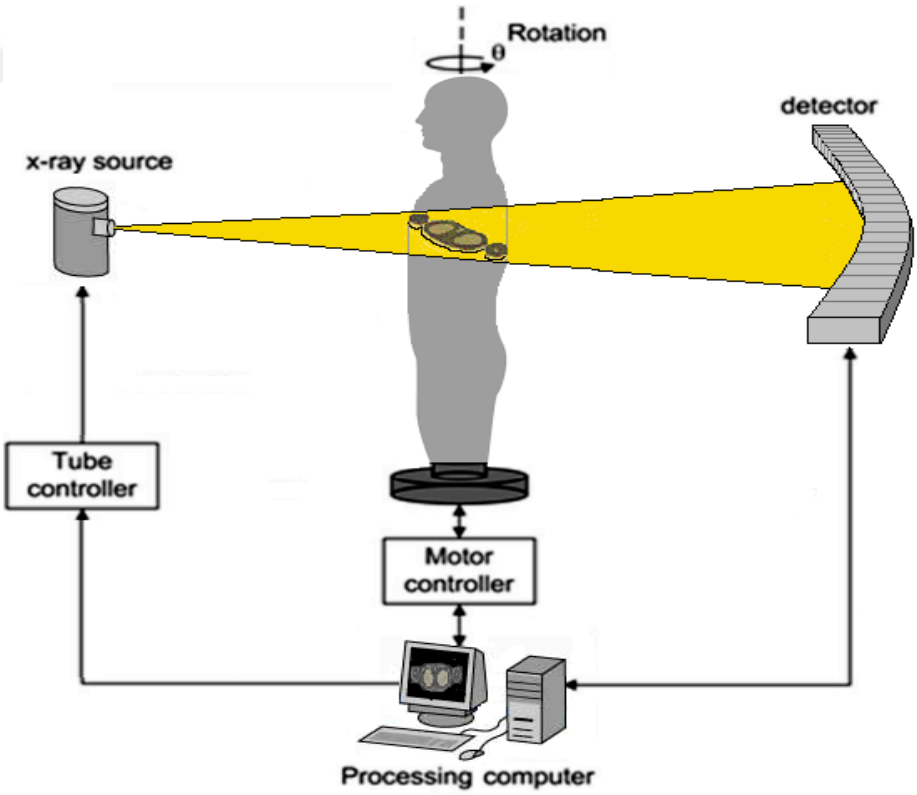

Figure 4.1 The basic elements and operations of the CT system

4.4 CT Image Representation and Parameters

Each information pixel creating the image is not actually two-dimensional. Indeed, it represents voxel structure which has a thickness and means volume element. Pixels which represent voxels in the obtained digital image carry CT number information. This parameter which is called as CT number represents the linear absorption coefficients. CT number is obtained by normalization of the linear attenuation coefficient of the tissue to the attenuation coefficient of the water [69, 70]. The formula of CT number is given at the equation 4.1.

$$\text{CT number} = \frac{(\mu_{\text{tissue}} - \mu_{\text{water}})}{\mu_{\text{water}}} * 1000 \qquad \textbf{(4.1)}$$

Where μ is the linear attenuation coefficients for water and tissue. The unit of CT number was called as Hounsfield Unit (HU) in memory of Hounsfield, who was nobel-winning physicist and found X-ray Computed Tomography, and values were shown on the scale of Hounsfield Unit [69]. According to Hounsfield scale, the given CT numbers to all voxels are positive for tissues whose concentrations are more than that of water, while they are in negative values for tissues whose concentrationa are less than that of water [8, 71]. HU values of the basic body material are listed in Table 4.1 [72]. Finally, voxels which take numerical values by Hounsfield scale are painted with black, white and shades of the gray in accordance with the values they get. In the Hounsfield scale, 0 value corresponds to the water, +1000 value is to the white color and -1000 value is to the black color [8, 71].

Table 4.1 The HU values of common body substances [72].

Substances	Hounsfield Unit (HU)
Air	−1000
Lung	−500
Fat	−100 to −50
Water	0
CSF	15
Kidney	30
Blood	+30 to +45
Muscle	+10 to +40
Grey matter	+37 to +45
White matter	+20 to +30
Liver	+40 to +60
Soft Tissue, Contrast	+100 to +300
Bone	+700 (cancellous bone) to +3000 (dense bone)

The CT number interval of Hounsfield scale is 2000 HU, but that interval can be up to 4000 HU in the advanced devices [8]. This range requires 4096 gray levels. However, the human eye can distinguish maximum range of 60 to 80 gray levels [69, 70]. Therefore, CT numbers of the desired region are compressed in the 60 and 80 gray level range. This processing is called windowing. All pixel values above the selected window are shown with white and ones under the window are shown with black. In Figure 4.2, the windowing process is shown. The center of window is mostly selected according to the average CT number of the desired region by the computer and applied to the image. In clinical practice such as the brain where the differences in the linear attenuation coefficients are very little, a narrow window is selected. While in clinical practice such as the thoracic region where the differences in the linear attenuation coefficients are very great, a wide window is selected [69].

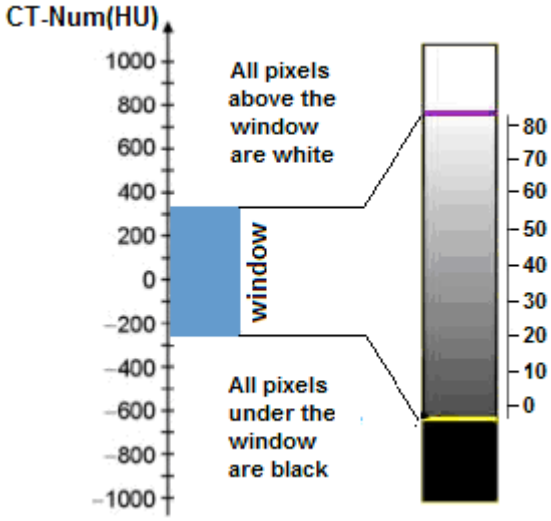

Figure 4.2 The process of "windowing", which maps a range of pixel values in window to a grayscale

4.5 CT's Generations

First-generation systems are with the single detector, and the X-ray is adjusted as a thin rod placed opposite the detector. They are systems which have quite slow-moving gantries because of the technology in that period. In the practice, tubes and detectors work with turning 180° around the patient with simultaneous linear and angular movements. Data collection and convertion to the image take a long time due to the computers with slow and insufficient memories in that period. Today, they are not in use [69, 73]. The first generation of CT is shown in Figure 4.3.

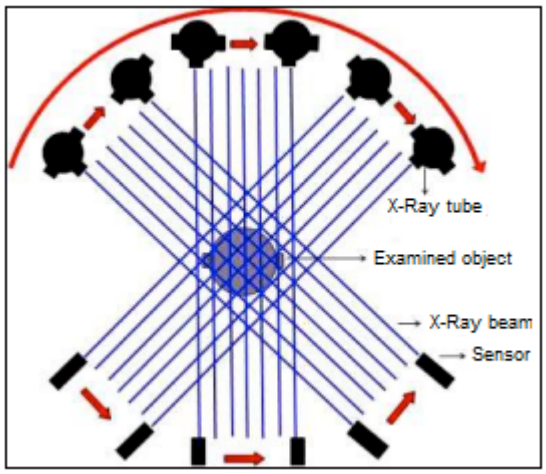

Figure 4.3 The first generation of CT systems [74]

The biggest difference of X-ray Computed Tomography systems, called also second generation, from the first generation is increase in the beams and their numbers. There is an array ionization detector filled with xenon gas instead of a single detector opposite the beam. Therefore, X-ray beam is in the form of narrow broom. Examination time is significantly reduced compared to the first generation system [69, 73]. The second generation of CT is shown in Figure 4.4.

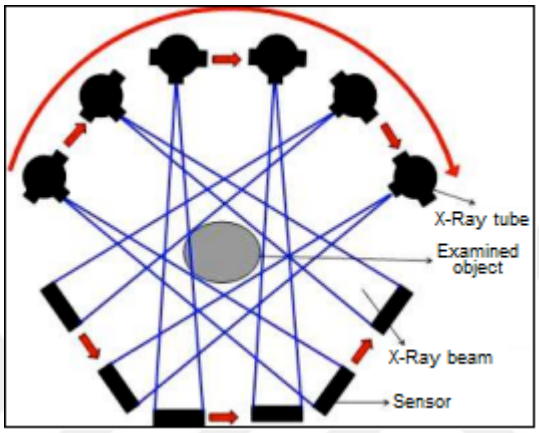

Figure 4.4 The second generation of CT systems [74]

In third generation systems, collimated X-ray is fan-shaped. X-ray beam passing through the patient falls on the detectors, whose number changes between 500 and 1000, filled with Xenon gas. In these systems, the detector and X-ray tube move mutual and simultaneous. They can make helical scanning as distinct from the first and second generations. While only brain CT could be carried out until this generation, other scannings have started to be performed by this generation. In addition, the angle of rotation rose to 360 degrees with this generation [69, 73]. The third generation of CT is shown in Figure 4.5.

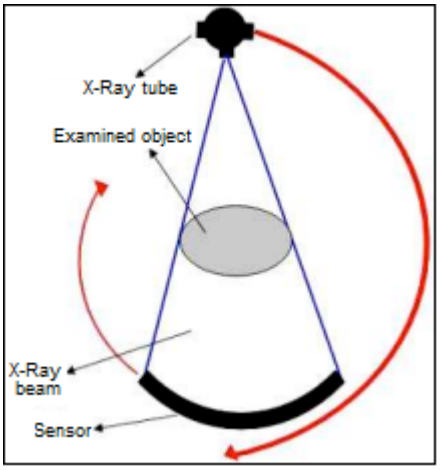

Figure 4.5 The third generation of CT systems [74]

In the systems called as fourth generation, static detectors in the form of circle are available in the gantry. In these systems, the detectors are constant and only X-ray tube acts around the patient. Some image defects, which appear on the third-generation system, such as ring artifacts do not appear in this generation. Cross-sectional images obtained from the patient are in the form of volume examination with the use of tubes producing continuous X-ray and the continuous movement of the patient table [69, 73]. The fourth generation of CT is shown in Figure 4.6.

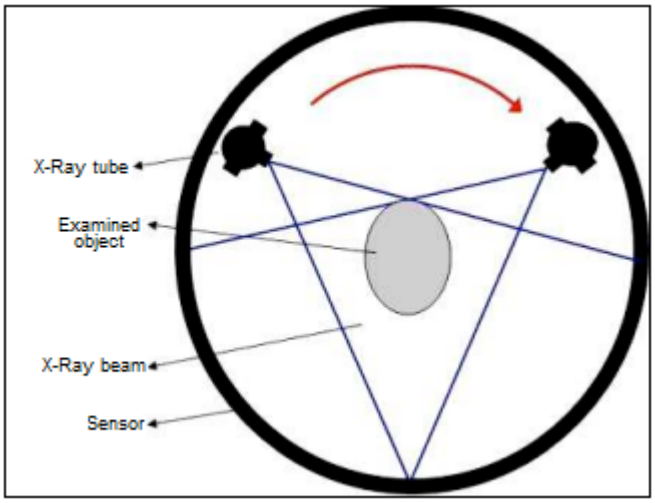

Figure 4.6 The fourth generation of CT systems [74]

The fifth generation is also called as Ultrafast. The movement of tube and detector is eliminated in this generation. Gantry space is surrounded by the anode ring. X-ray

tube is replaced with strong electron beam. At the present time, the fifth generation devices, which have not entered into widespread use yet, are in the development stage [73].

4.6 In Clinical Uses of CT Devices

CT device is one of the most common used diagnosis techniques in radiology. CT works in accordance with ability and opportunities provided by the X-ray, because it uses X-ray principles as the basic. A large amount of X-ray applied to human body is absorbed due to Ca (Calcium) element which is available intensive in the bone tissue. This case offers contrasting capability to CT device in a broad sense, and it means the diagnostic superiority in the bony tissue for CT device. As a result, CT device has a high imaging capability in the skull and spine regions. Besides, X-ray can easily pass with very little absorb or without any absorb from the soft tissues where Ca element is available no or very little. As a result of this, CT scanners have the limited contrasting ability in the soft tissue such as the liver, intestine [8, 67].

4.7 CT's Clinical Advantages

1. One of the most important advantages of CT is its ability to evaluate the intensity of the lesions between -1000 and +1000. Minuses which are close to zero (-10, -20) represent fat tissue, pluses which are close to zero (+10, +30) represent fluid structures, and +300, +350 show calcified structures. The bone structure which is the most intense structure is determined by +1000.
2. CT is extremely successful at making the bony tissues contrast.
3. CT shows quite clearly the shape and layout of organs, soft tissues and bones.
4. CT scans allow better evaluation of the diseases with helping on differential diagnosis of a simple cyst (pouch-shaped formation in which there is liquid or semi-liquid substance) and solid tumors (tissue mass occuring).
5. CT helps on the evaluation of the spread of the cancer with creating images which are much more detailed than direct radiography.

6. CT makes it possible to evaluate many parts of the body like the brain, which can not be shown by direct radiography.
7. CT provides earlier and more accurate diagnosis of many diseases than other imaging methods. Diseases can be cured better and faster when they are diagnosed early, therefore CT has helped the doctors to save many lives with its superior properties.
8. CT is preferred commonly, because it can be performed fastly and can examine many different organ systems in minutes [75].

4.8 CT's Clinical Disadvantages

1. Computed Tomography contains X-ray, namely radiation. Although imaging can be maden with low doses and suitable dose adjustment based on the patients by courtesy of developing technology, the indications should be well identified and the patient selection should be made accurate for Computed Tomography.
2. CT is prohibited for the patients (pregnant women, etc.) who are inconvenient to exposure to radiation, because the radiation which is emitted and penetrates to body during tomography is at the very high rate.
3. CT is weak to make soft tissue contrast. Therefore, it is insufficient to determine the tissue specificity.
4. Metallic foreign objects constitute artifacts.
5. It is impossible to distinguish different pathological benign lesions with CT. An abscess may be seen in the same appearance with malignant tumor or hematoma. Therefore, discrimination of whether a solid mass is benign or malignant can not be made [66, 76].

CHAPTER 5

APPLICATION OF IWS ON BIOMEDICAL IMAGES

The use of medical imaging systems for diagnosis and treatment is increasing in the world. Therefore, imaging equipments has been in a continuous change and development until the present day as a result of intensive research and development studies performed on the medical imaging systems by the researchers. Unlike this development in imaging systems, studies on helper programs for the analysis and interpretation of obtained images has not been carried out sufficiently. Whereas, imaging techniques like CT are diagnostic tools including huge amount of the information which radiologists have to analyze and make a comprehensive assessment in a short time about. Therefore, the applications which help radiologists evaluate the CT images are still needed [77].

In the radiology, computer-aided diagnosis (CAD) are helpful systems which can develop doctors' diagnostic skills and reduce the time required for accurate diagnosis as helping them interpret the medical images [77, 78]. CAD systems including image processing algorithms have the potential to highlight possible diseases having abnormal apperance and to detect lesions (or nodules) for CT studies [79].

In the scope of this thesis, a computer-aided diagnosis system depending on Image Weight Signal (IWS) tecnique, which is proposed for detection, counting and sizing of the diseased regions, is developed. Presented system detects, counts and sizes lung nodules through CT images as semi-automatic and classifies the lungs into healthy and diseased.

5.1 Application of IWS for Lung Nodules in CT Images

Lung nodules are lesions which settle in the lungs and whose diameters are smaller than 4 cm. They may be a residue remaining after an infection passed, a benign lung tumor or lung cancer, or they may occur with the spread of another organ cancer to

the lungs [80]. Lung nodules are structures that can be seen in the chest radiograph, and have round or oval appearance around the lungs. Nodules which are greater than 1 cm are called as large nodules and nodules which are smaller than 1 cm are called as small nodules, while nodules which are greater than 3 cm are called as mass [81].

Data used in this presented application of research were obtained from LungCT-Diagnosis collection, sponsored by Moffitt Cancer Center (Tampa Florida), of The Cancer Imaging Archive (TCIA) [82]. Data collection contains 61 patients and each ones' image series. All the images are diagnostic contrast enhanced CT scans. They have a size of 512 × 512 pixels and are stored in Digital Imaging and Communication in Medicine (DICOM) format. Scanning window width is 400.0, so FOV value used to obtain area information in mm^2 is 400x400 in the application. Slice thickness is variable between 3 and 6 mm. Diagnosis were done for all patients at the prior to surgery.

5.2 Methodology of the Application

The application aims to detect lung nodules in lung CT images, to separate from other tissues, to calculate the number and area information of the nodules with IWS method. The methodology followed for these purposes is shown in the flow diagram presented in Figure 5.1.

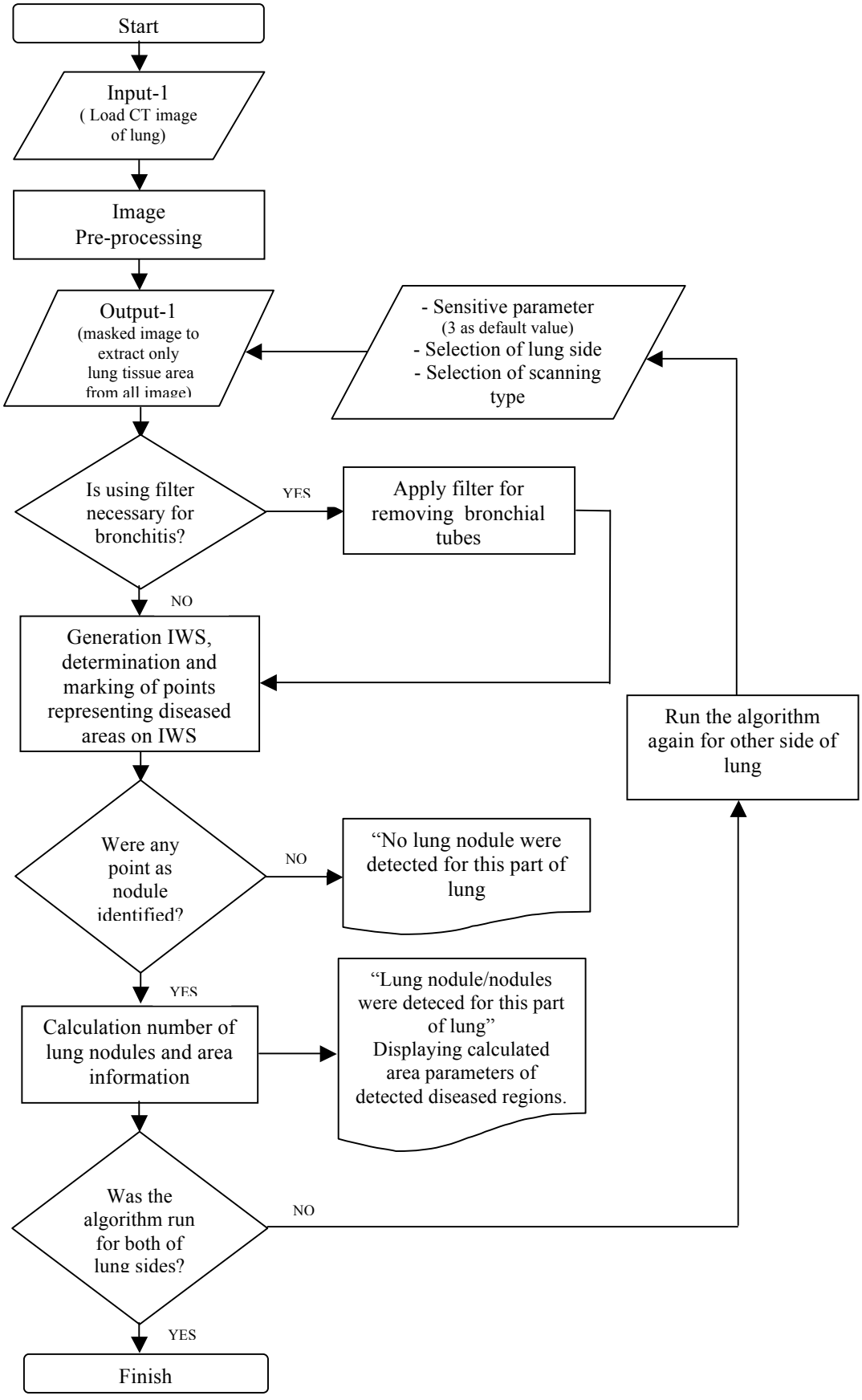

Figure 5.1 Flow chart for steps and processes of application

5.2.1 Detection and Extraction of Lung Nodules

Image analysis includes producing quantitative information in terms of the measured properties about the objects in the image. However, the images are often complex, noisy and full with artefacts. Therefore, the image must be cleaned to extract meaningful quantitative information from the image. The aim of pre-processing including many image processing steps is to clean medical images obtained generally with artefacts and to make them ready for image analysis. Consequently, medical images loaded as the input are put to pre-processing in presented application. In the pre-processing step, a series of segmentation and morphological processes are implemented in succession and a mask is formed as a result. When lung CT images are masked by the mask created from itself, desired lung tissue is obtained as purged from unwanted fat, skin, bone tissues surrounding it. Thus, the image is maden ready for analysis.

The content of the preprocessing used in the application is described step by step and the effect / function of each step on the image is shown in Table 5.1

Table 5.1 Steps of pre-processing.

Input data for the pre-processing is one of lung CT scan's slices containing nodule/nodules. Firstly the image is converted to gray level image.	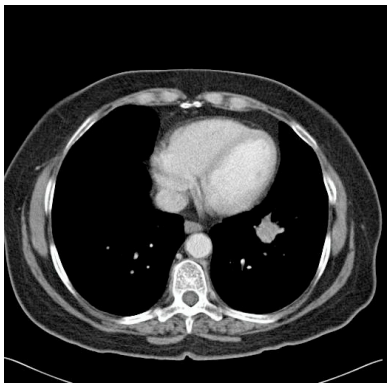
Treshold segmentation process is applied to the image converted into gray level. With this process, gray level image is converted to black and white level, pursuanting to the threshold value.	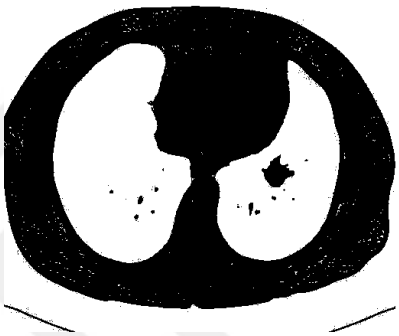
White environment frame surrounding the body in the image is converted to black and the shape of the lung tissue in the examining slice is extracted.	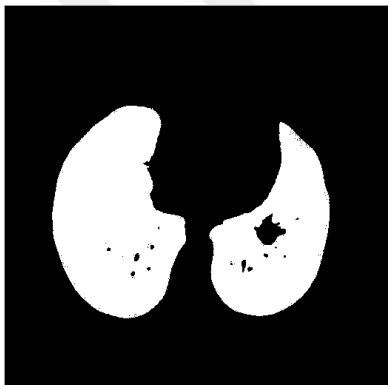
In order to convert the obtained image to the mask form, the white pixels representing the lungs are converted to black, while other pixels are converted to white. However, black pixels which represent the structure of a bronchus or nodule and are within the lung boundaries are remaining as black, because they are located in the lung structure. Thus, lung mask belonging to individual is formed.	

The original CT slice image is masked with produced individual lung mask. Thus, undesired structures such as bone, skin are removed from the image and only lung structure is obtained.	
For the study convenience, the image, whose lung structure is extracted, is divided into two parts as the right and left lung. Thus, both lung sides can be investigated and analyzed separately.	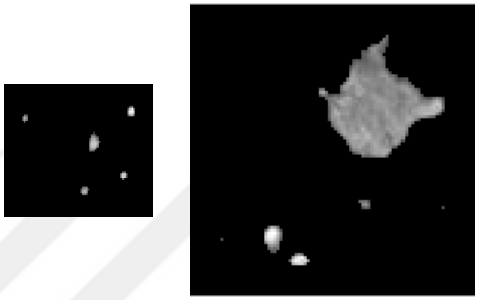

Input CT image is obtained as two separate images for the left and right lungs after pre-processing step. Other structures, which are located outside the lung area, such as bone, muscle, skin are removed in these created images, because they are not parts which will be investigated. In the images, there are only the bronchial tubes and lung nodules, if any, which are located within lung structure. Mostly, bright pixels represent bronchial structure, the community of gray pixels which are non-glossy represents nodules, and black pixels which also belong to the background represent the lung tissue in the images. However, only lung nodules are needed in the thesis. Therefore, the bronchial tubes are removed from the right and left lung images by application of a filter. Filtering process of the bronchial tubes is shown in Figure 5.2. Thus, images containing only nodules are obtained and would be ready for the IWS analysis.

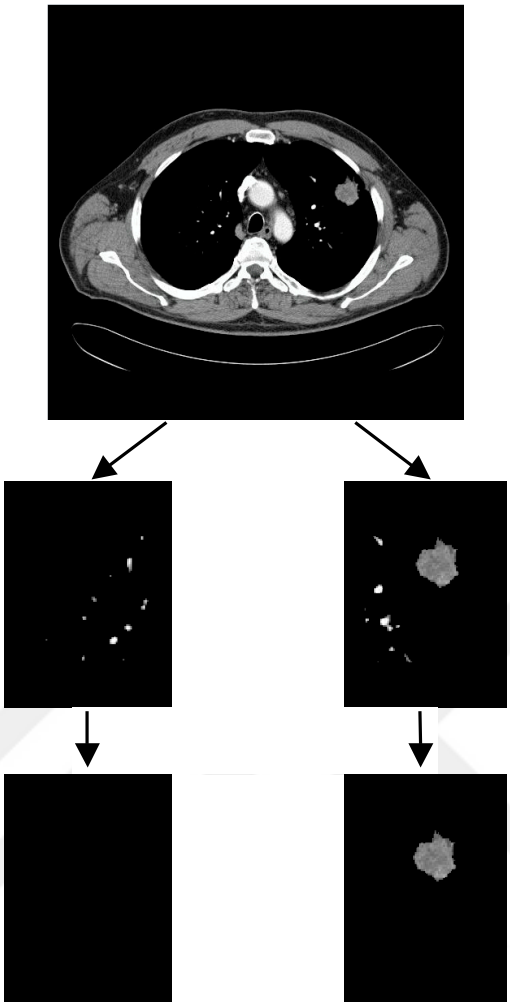

Figure 5.2 Filtering process of the bronchial tubes in the the right and left lung images obtained with pre-processing steps from input CT image

5.2.2 Counting, Sizing and Classification of Lung Nodules

IWS analysis is performed on the left and right lung images by two different scanning methods, including horizontal or vertical scanning. In the application, the selection of scanning type is belonging to the user and it is maden according to the location and sequence of lung nodules, namely detected diseased regions, with each other. The horizontal scanning is used if nodules are located on the horizontal axis. Similarly, the vertical scanning method is selected if nodules are located on the vertical axis. Both scanning methods can be used if they are cross-listed. The selection of scanning method to obtain IWS affect the accuracy of the results produced by algorithm.

An example for the type selection's effect on the accuracy of the results produced is shown in Figure 5.3. In the example given below, the nodules detected successfully with pre-procesing on the image are detected and sized by IWS technique with horizontal and vertical scanning. Nodules in the image are located in the vertical direction. Hence, nodules can be successfully decomposed, and their area information is calculated accurately and separately by IWS with vertical scanning. However, nodules can not be successfully separated by IWS with horizontal scanning. The reason of this is that three separate nodules is perceived as a single nodule because of their location structure on the vertical plane during the horizontal scanning. As a result, total area information of three nodules is produced as only one nodule information. It means that production of accurate result depends entirely on the choice of suitable scanning type.

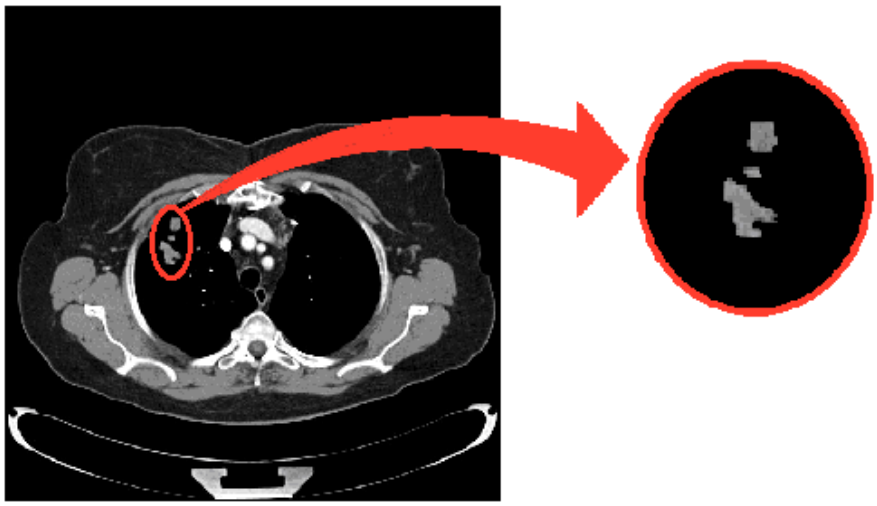

(a)

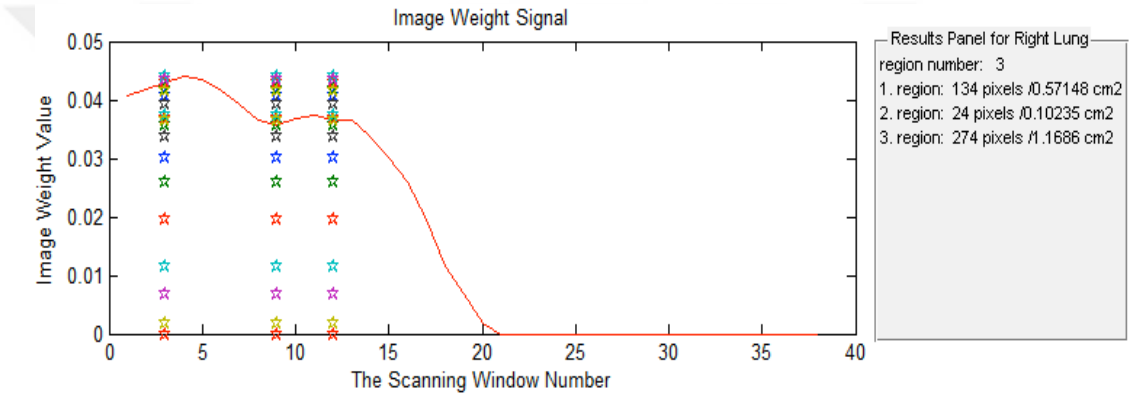

(b)

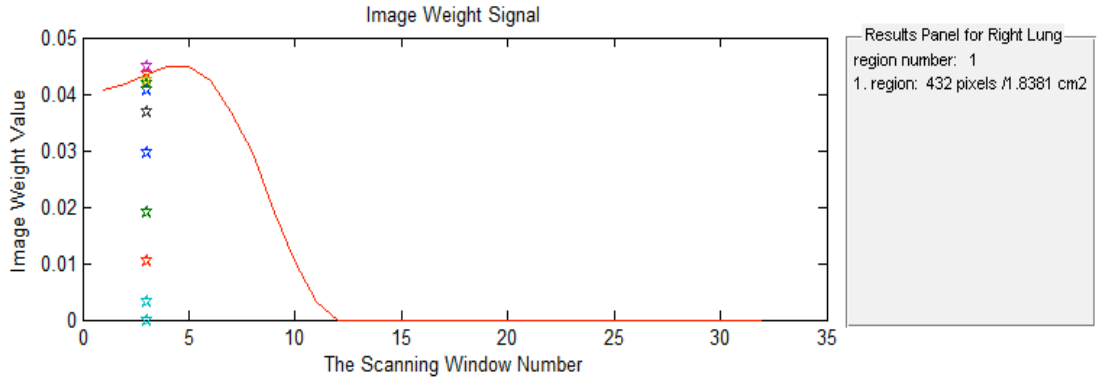

(c)

Figure 5.3 The IWS and results of IWS analysis on the (a) lung CT image with nodules by the (b) vertical scanning and (c) horizontal scanning

In Figure 5.4, alignments of detected nodules in the horizontal and vertical axis are shown. Because of these alignments of the nodules, all nodules can be sized accurately (134, 24 and 274 pixels) with the vertical scanning, while size information can not be calculated (432 pixels) with horizontal scanning.

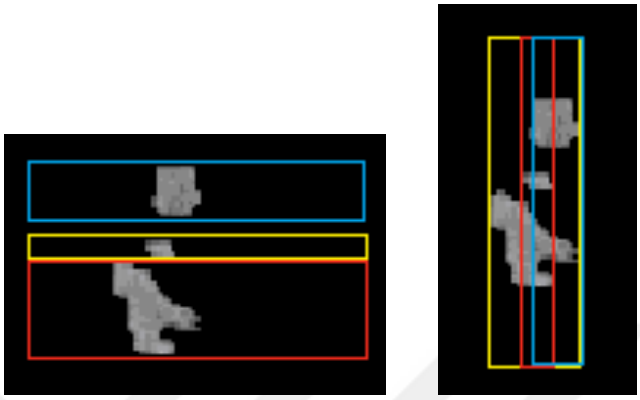

(a) (b)

Figure 5.4 (a) Vertical alignment and (b) horizontal alignment of the detected nodules

An another example for the type selection's effect on the accuracy of the results produced is shown in Figure 5.5. In the example given below, the nodules detected successfully with pre-procesing on the image are detected and sized by IWS technique with horizontal and vertical scanning. Nodules in the image are located in the horizontal direction. Hence, nodules can be successfully decomposed, and their area information is calculated accurately and separately by IWS with horizontal scanning. However, nodules can not be successfully separated by IWS with vertical scanning. The reason of this is that three separate nodules is perceived as a single nodule because of their location structure on the horizontal plane during the vertical scanning. As a result, total area information of three nodules is produced as only one nodule information. It means that production of accurate result depends entirely on the choice of suitable scanning type.

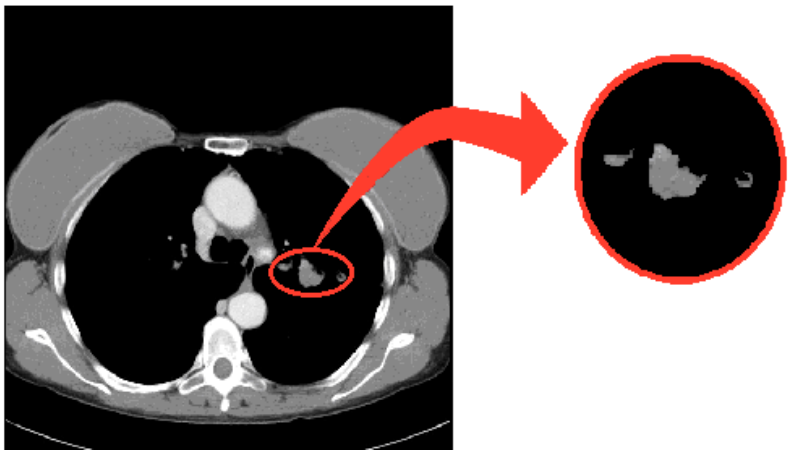

(a)

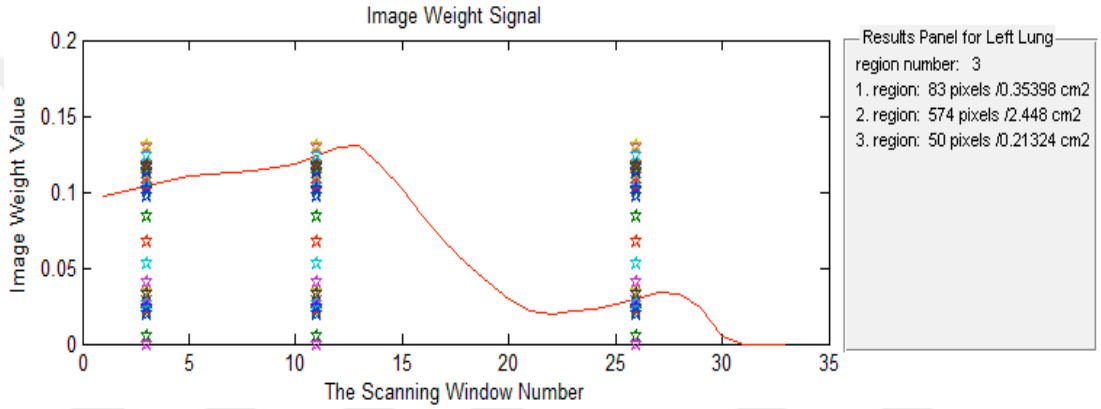

(b)

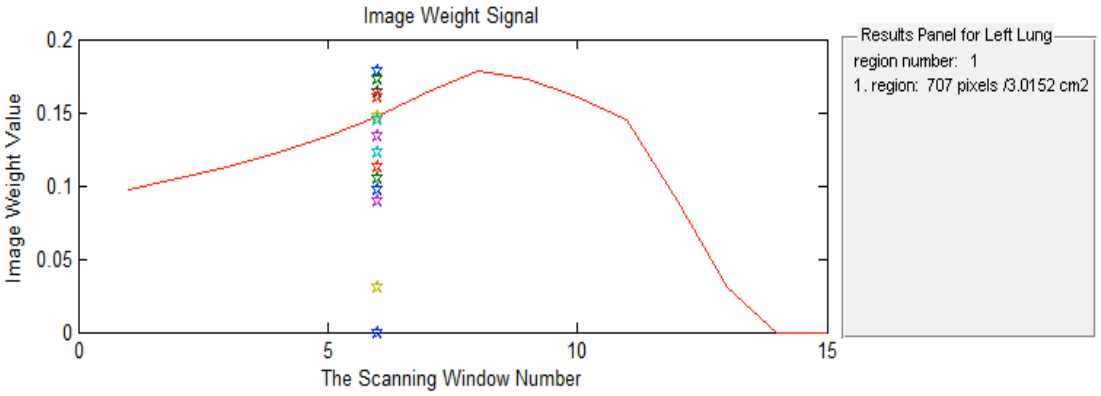

(c)

Figure 5.5 The IWS and results of IWS analysis on the (a) lung CT image with nodules by the (b) horizontal scanning and (c) vertical scanning

In Figure 5.6, alignments of detected nodules in the horizontal and vertical axis are shown. Because of these alignments of the nodules, all nodules can be sized accurately (83, 574 and 50 pixels) with the horizontal scanning, while size information can not be calculated (707 pixels) with vertical scanning.

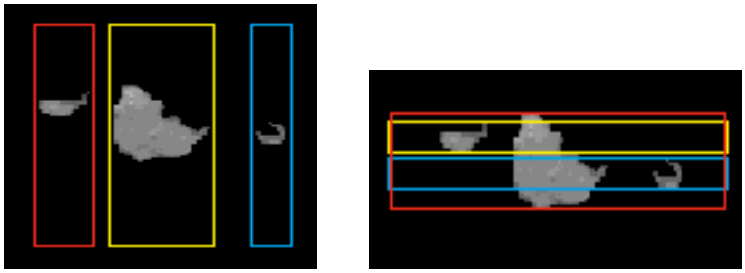

(a) (b)

Figure 5.6 (a) Horizontal alignment and (b) vertical alignment of the detected nodules

In the developed application, the number and area information of the nodules can be easily obtained with the selection of appropriate scanning type for the IWS. Besides, " no diseased region was detected! " is displayed as result in the case of the absence of lung nodules. In Figure 5.7, an example of obtained IWS and its results in the absence of lung nodules is shown.

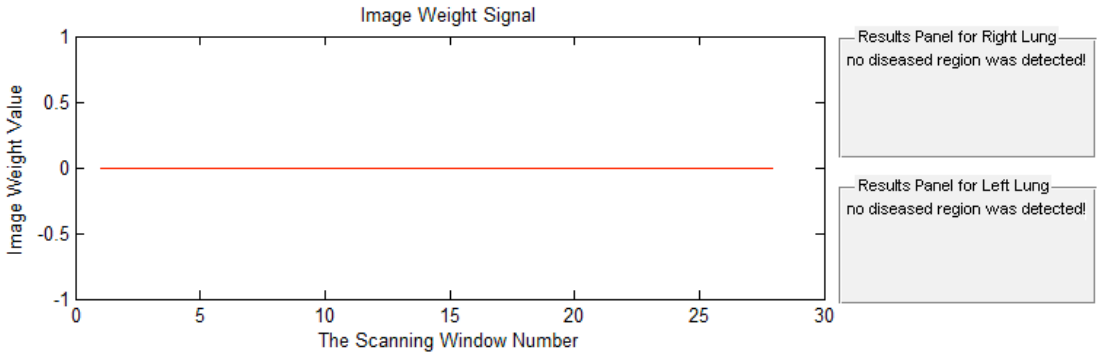

Figure 5.7 The IWS and results of IWS analysis on the lung CT image without nodule for right and left lungs

5.3 Application of Graphical User Interface

In the study, a CAD system based on the IWS technique proposed for the counting and sizing of the objects in the binary image were developed for the application. With the aim of providing the users to be able to use the system without the necessity of reading algorithm code, the Graphical User Interface (GUI) is designed in MATLAB for the developed CAD system. In addition, this interface provides great convenience for the users about patient selection, display of original and processed images, scanning type selection, display of produced IWS, representation of the number and area information results of the nodules. In Figure 5.8, window display of the designed user interface is presented.

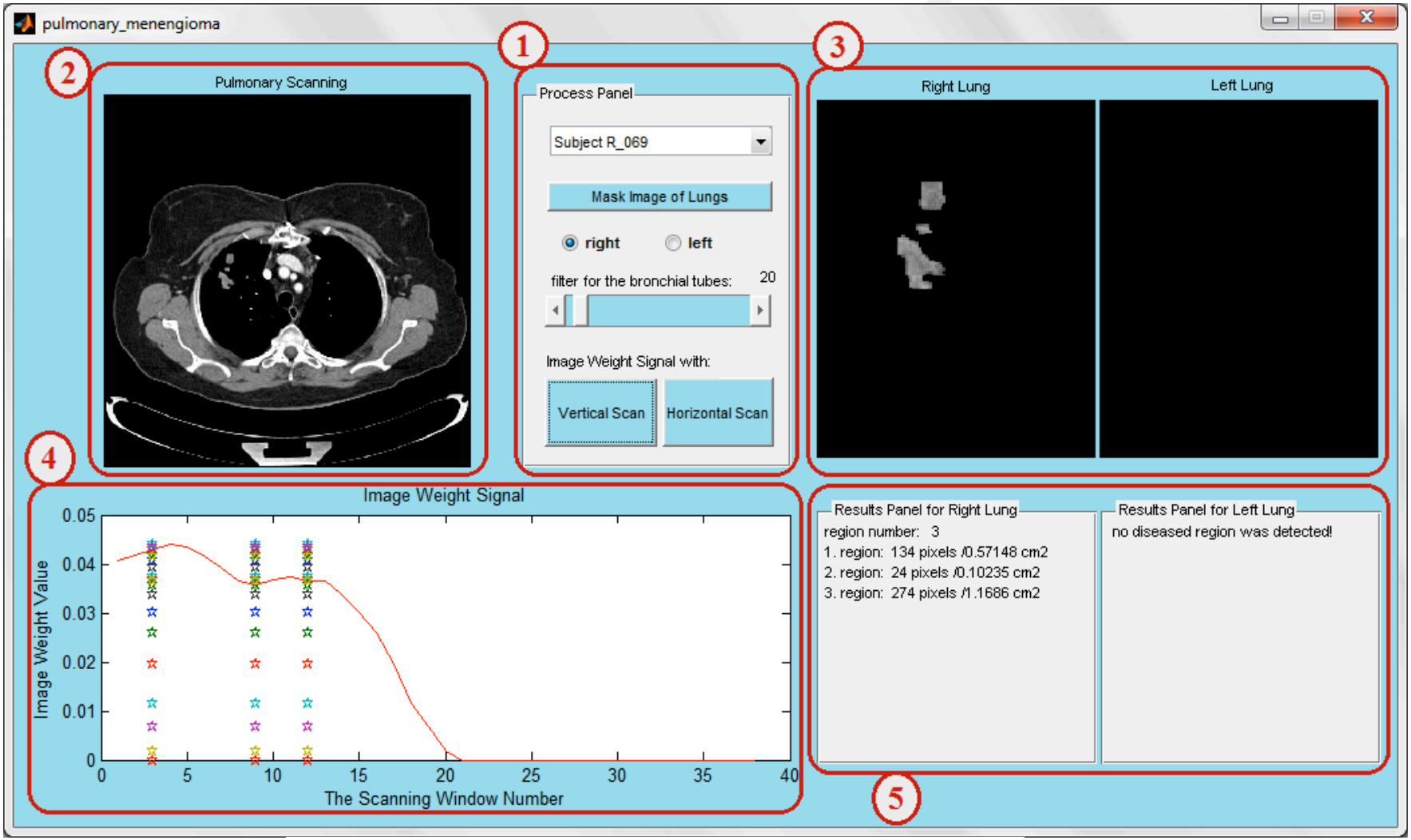

Figure 5. 8 Designed graphical user interface for CAD system

There are 5 basic sections, which are marked with red frames, in the designed interface. The user can make process and be effective in the only first section. Other parts except first section are related to representation of data and results.

Sections and their functions:

1. This section contains a process panel for the user. It is part in which the users can be effective and manage the application. This section containing the process panel and its subsections is shown in Figure 5.9.

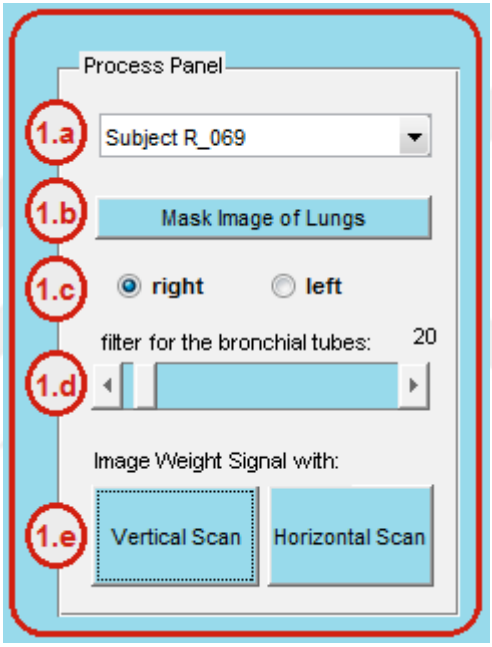

Figure 5.9 Process panel and its subsections

1.a. This part of the first section is a pop-up menu. The user performs the selection of desired patients from this menu. When patient selection is done by user, system automatically loads CT cross-sectional image belonging to selected individual, performs pre-processing step on the image, performs the display of the original CT image and the right and left lung images obtained as result for the observation of the user on the interface. An example of the patient selection done by pop-up menu is shown in Figure 5.10.

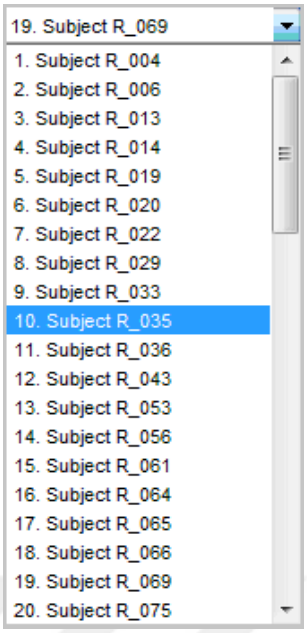

Figure 5.10 Patient selection by pop-up menu

1.b. This part of the first section is a push button. It is not a compulsory step in the work flow of the system and does not include a process. It is a tool used when the user wants to see the individual lung mask obtained in the pre-processing step. This button displays mask image in an opened new figure window and allows user to observe the structure of the lung mask. An example of figure window opened with this button and mask image displayed in it is shown in Figure 5.11.

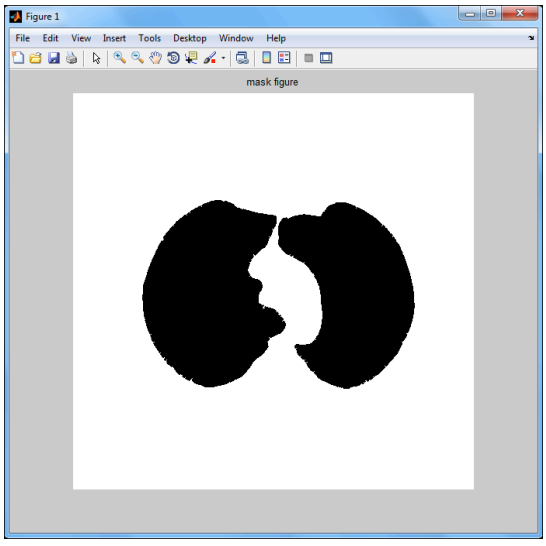

Figure 5.11 Lung mask image on the figure window opened by 1.b push button

1.c. This part of the first section includes two radio buttons. The user performs the selection of the right or left lung image which is desired to be examined. Whole processes performed after this selection are realized on the image selected in this step. After ending the examination of the selected lung image, the other part of lungs is also examined with selection of other radio button. However, if the examination of only the right or only left lung is enough, there is no need for the second selection.

1.d. This part of the first section is a slider. The user can adjust the parameter of the filter applied to remove the bronchial tubes in the selected right or left lung image with this slider. At the each parameter value set by the slider, the filter's effect on the image can be observed on the third section of interface by the user, so the most appropriate parameter value can be easily chosen. An example of the slider usage's effect on the image and the determination of the optimal parameter value is shown in Figure 5.12.

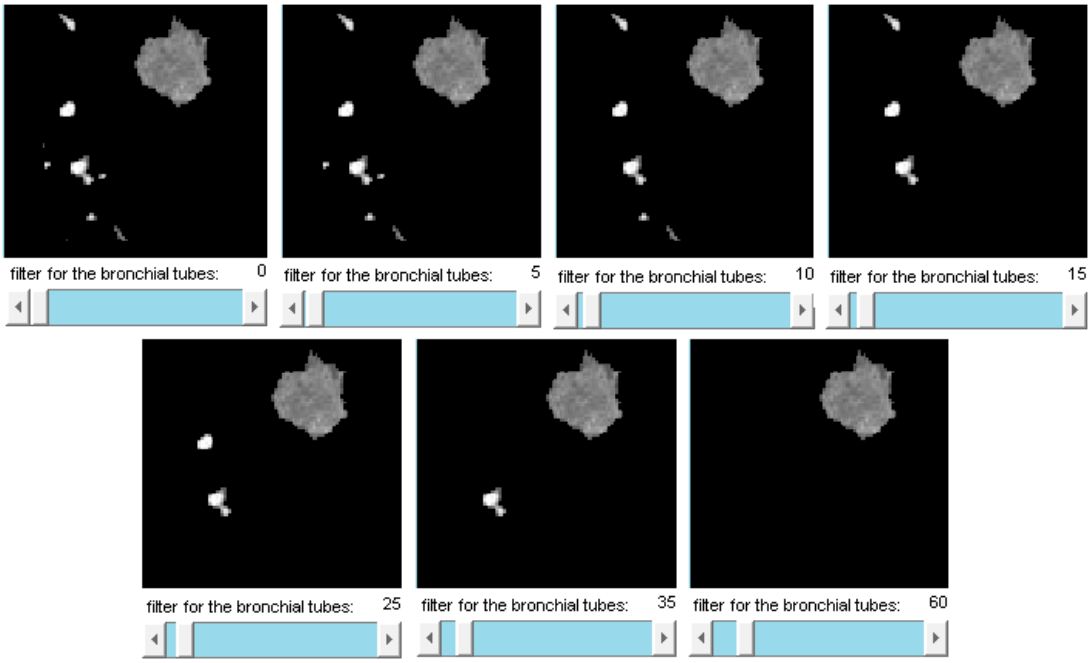

Figure 5.12 Usage of slider and its effects on the image

1.e. This part of the first section includes two push buttons. User performs IWS analysis with the vertical scanning by former and IWS analysis with the horizontal scanning by latter on the image selected with 1.c and filtered with 1.d. The selection of scanning type depends on the user. When these buttons are pressed, the system automatically carries out the IWS analysis with scanning type which the pressed button represents, also the obtained IWS and the calculated results are presented to the user on the interface.

2. This section consists of an axes. The presentation of the raw lung CT image belonging to the selected individual with 1.a is performed automatically in this section. The user can obtain first impression about CT image with this display. The image which is set in this section after patient selection, is not affected from the performed processes and it remains constant throughout the analysis. This section is given in Figure 5.13.

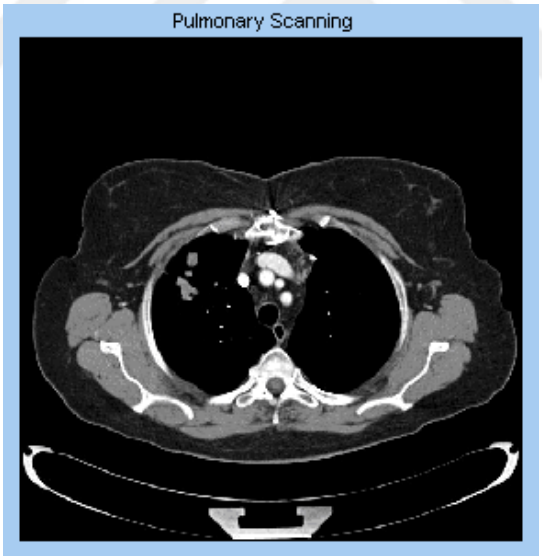

Figure 5.13 Presentation of CT image on section 2

3. This section consists of two axes. Representation of the right and left lung images obtained with the pre-processing step is performed automatically in this section. Right lung image is located in the first axes, while left lung image is located in the second one. These images are affected from the parameter value of the filter which is in the section 1.d, and the effects of the

filter on the images can be observed immediately. An example of representation of divided lung images is presented in Figure 5.14.

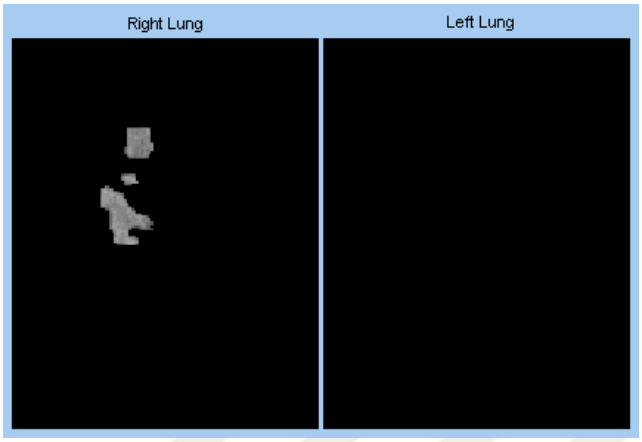

Figure 5.14 Presentation of pre-processed and separated lungs' images on the section 3

4. This section consists of an axes. When one of the push buttons located on 1.e is pressed, the display of weight signal obtained from the IWS analysis performed with the scanning type, which the pressed push button represents, is realized in this section. An example representation of weight signal is presented in Figure 5.15.

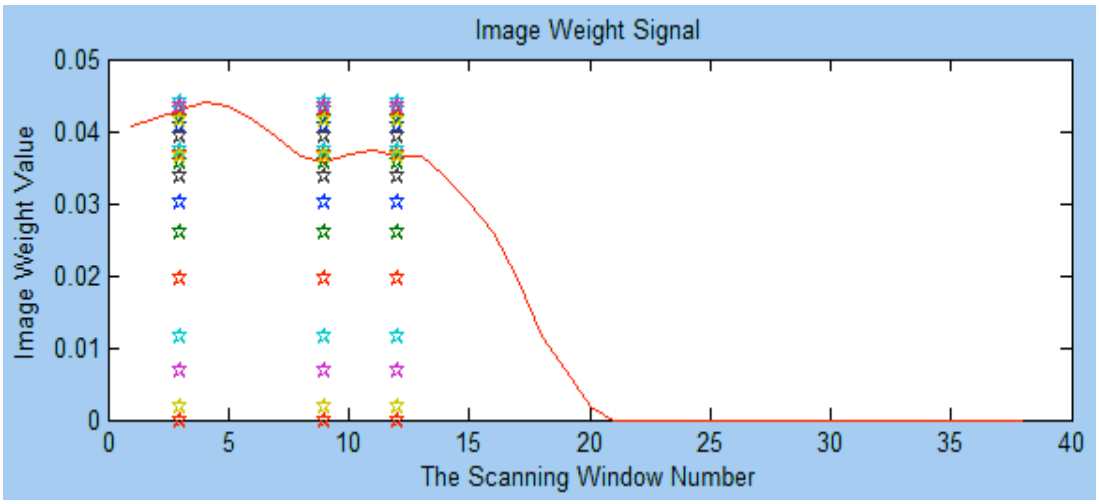

Figure 5.15 Presentation of IWS on the section 4

5. This section consists of two panels on which quantitative results obtained with IWS analysis is presented to the user. Former is for the results of right lung and latter is for that of left lung.

5.a. In this part of section 5, quantitative results of IWS analysis performed on the right lung image is demonstrated. An example display of the quantitative results calculated for the right lung is presented in Figure 5.16.

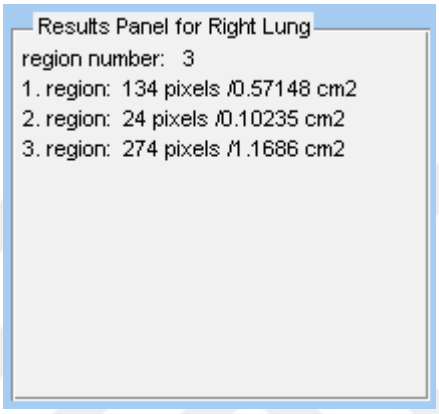

Figure 5.16 Presentation of quantitative parameters on the section 5.a

5.b. In this part of section 5, quantitative results of IWS analysis performed on the left lung image is demonstrated. An example display of the quantitative results calculated for the left lung is presented in Figure 5.17.



Figure 5.17 Presentation of quantitative parameters on section 5.b

CHAPTER 6

CONCLUSIONS AND FUTURE WORKS

Medical imaging is one of the main areas aiming the application of the engineering principles in the biology and medicine fields. Cumulative advances in medical imaging science provide a significant convenience and improvement on the medical diagnostic, prognosis (to predict the course of disease and how long will continue), and treatment. However, the accuracy of image analysis results applied in medical data is as important as the reliability of the data acquisition process at least. The analysis of medical imaging data requires the application of techniques containing the image processing and analysis which is one of the key issues for the engineering and computer sciences.

The main purpose of this thesis was to develop an analysis technique (IWS) for the calculation of the number and separately area information of desired objects/regions in a black-white image. Moreover, the creation of the CAD framework allowing the developed analysis method's implementation on the lung CT images was also aimed.

In this thesis, an extensive perusal was done in the image processing and analysis literature, and a wide background about it was presented. Object counting methods were examined deeply till the mathematical principles and their applications were carried out by their written algorithms. As well as object counting process performed by these methods, IWS analysis method which performs also object sizing process has been developed. This analysis technique's an application in the medical field, where area parameter is so important, has been presented. In this application developed for lung CT images, lung nodules were detected and extracted from the image with pre-processing; the number and area information of the nodules were calculated with IWS analysis technique; the classification of the lungs into healthy or diseased were maden based on these produced results. LungCT-Diagnosis data set containing 61 patients was used for this application [83]. The performance of the

classification, which was carried out based on the results of the IWS method, was evaluated by calculating the different measurements given below:

$$\text{Sensitivity}(\%) = \frac{TP}{TP+FN} * 100 \quad \textbf{(6.1)}$$

$$\text{Specificity}(\%) = \frac{TN}{FP+TN} * 100 \quad \textbf{(6.2)}$$

$$\text{Accuracy}(\%) = \frac{TP+TN}{TP+FN+TN+FP} * 100 \quad \textbf{(6.3)}$$

TP, TN, FN and FP express true positive, true negative, false negative and false positive respectively [10]. Performance measures of the classification performed in the application are given in Table 6.1. Right and left lungs of the individuals were evaluated separately in the calculation of the measure values.

Table 6.1 Classification performance measures.

	Accuracy	Sensitivity	Specificity
Classification of LungCT-Diagnosis Collection as normal and abnormal by IWS results	92%	86%	98%

In a study carried out by Magdy et all. (2015), automatic classification of normal and cancer lung CT images were performed with four different classifiers: *K*NN, SVM, naïve Bayes and linear classifiers [10]. The computed accuracy, sensitivity and specificity parameters were obtained respectively 64%, 55%, 72% for *K*NN, 90%, 85%, 97% for SVM, 82%, 82%, 82% for naïve Bayes and 95%, 94%, 97% for linear classifier. It can be easily noticed that performances of *K*NN and naïve Bayes are much worse than that of the proposed system in terms of accuracy, sensitivity and specificity. The performance of linear classifier is a bit better than the classification performed in the proposed system, while that of SVM is a bit worse.

Misclassification which is made for some lungs in the application do not take its source from results obtained with IWS. The cause of misclassification is wrong mask production for the lungs in the pre-processing step because of nodule which is connected with the lung border. Hence, nodule structure is removed from the masked image together with the unwanted tissues and so, the classification based on the results of IWS produces wrong result. An example of wrong lung mask production causing misclassification is shown in Figure 6.1.

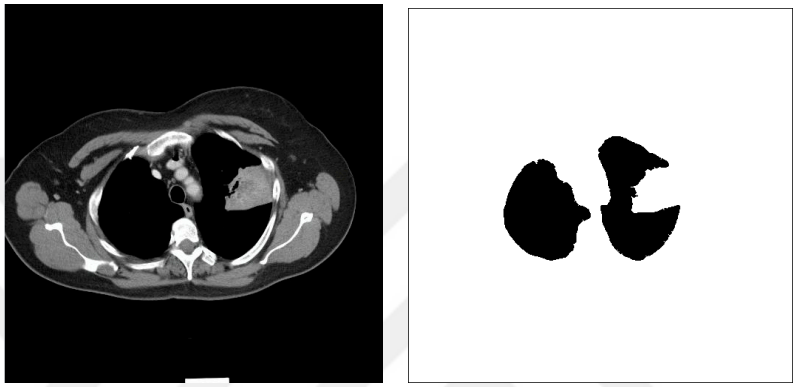

Figure 6.1 An example of the wrong mask production

Successful performance and accuracy of the classification carried out with developed IWS method reflect also the accuracy of other produced outcomes such as the nodule number, area parameter. Quantitative results, which are the number and area information of nodules, were obtained with about 88% accuracy in the application, while it reached an accuracy of almost 95% if individuals whose lung mask produced wrong excluded.

Medical image analysis may help and guidance to the radiologist for diagnosis, treatment plan and the follow-up phase of the treatment with the results produced by analysis techniques. In the application presented in the thesis, obtaining of quantitative measure parameters belonging to detected diseased regions can help doctors select treatment with interpreting results, and can make the follow-up process of the disease more efficient and easier by means of comparing results.

In the thesis, CAD framework was created for developed medical application. The MATLAB software platform was used to form CAD system and graphical user interface (GUI) was designed within the context of CAD. This designed CAD system allows practises with putting medical image processing and analysis methods into a sequence; supports radiology specialists on the diagnosis, treatment planning and follow-up with the help of produced information; and offers the user convenience for making it possible to be used by not only engineers, but also field professionals.

In this thesis containing interdisciplinary studies, developed analysis technique is open to be improved for the works which will be performed by others in the future, because its algorithm was presented in the code system. Method has a requirement, which objects/regions have to be in a certain alignment, to produce accurate results. New codes can be added and necessary parts can be modified to overcome this limitation and to develop method further. Written algorithm can calculate the number and area parameters of the objects as the result. Besides it, the additional codes may be added to calculate also other parameters such as width and height of desired objects or regions. Created system may be improved for convertion from semi-automatic to fully automatic. In addition, method's applications can be developed in not only medical field, but also other areas such as product quality control systems. The designed user interface is always open to improvement. The usage of interface may be made even easier with working more deeply on interface, and more simple appearance may be provided for it. Moreover, .NET application of performed study can be developed.

REFERENCES

[1] Demirci, F., *"Filyos Havzasındaki Sediment Birikim Alanlarının Uydu Görüntü Verileri ve Sayısal Arazi Modeli ile Analizi",* Thesis (M.Sc), İstanbul Teknik University, Institute of Science and Technology, Department of Geomatics Engineering, 2008.

[2] Karagülle, F., *"Destek Vektör Makinelerini Kullanarak Yüz Bulma",* Thesis (M.Sc), Trakya University, Institute of Science and Technology, Department of Computer Engineering, 2008.

[3] Cengizler, Ç., *"A Fluid Dynamics Based Image Segmentation Approach and Pap-Smear Image Data Classification",* Thesis (M.Sc), Çukurova University, Department of Computer Engineering, 2013.

[4] Ashir, A.M., *"Simulation of FPGA-Based Image Processing System for Quality Control and Palletization Applications",* Thesis (M.Sc), Mevlana (Rumi) University, Department of Electrical-Electronics Engineering, 2014.

[5] Sabancı, K., and Aydın, C., *"Görüntü İşleme Tabanlı Hassas İlaçlama Robotu",* Tarım Bilimleri Dergisi – Journal of Agricultural Sciences, Vol. 20, pp. 406-414, 2014.

[6] Fidan, U., and Süzme, N.Ö., *"Küf Gelişiminin Görüntü İşleme Teknikleri ile Analizi",* Afyon Kocatepe University, Journal of Science and Engineering, Vol.15, pp. 13-21, 2015.

[7] Klinder, T., Ostermann, J., Ehm, M., Franz, A., Kneser, R., and Lorenz, C., *"Automated Model-Based Vertebra Detection, Identification, and Segmentation in CT Images",* Journal of Medical Image Analysis, Vol. 13, pp. 471–482, 2009.

[8] Yüksel, H., *"Medikal Görüntü İşleme İçin Fraktal Geometri Kullanarak Üç Boyutlu Modelleme ve Hızlı Prototipleme Yazılımının Geliştirilmesi",* Thesis (M.Sc), Süleyman Demirel University, Institute of Science and Technology, Department of Electronics and Computer Education, 2010.

[9] Yıldırım, M.S., *"Analysis of Magnetic Resonance Images of Patients Having Spontaneous Spinal Cerebrospinal Fluid Leaks and Intracranial Hypotension Using Computerized Image Processing Methods"* Thesis (M.Sc), Fatih University, Electrical-Electronics Engineering, June 2011.

[10] Magdy, E., Zayed, N., and Fakhr, M., *"Automatic Classification of Normal and Cancer Lung CT Images Using Multiscale AM-FM Features",* International Journal of Biomedical Imaging, Vol. 2015, No. 230830, 2015.

[11] Madisetti, V.K., and Williams D.B., *"Digital Signal Processing Handbook",* CRC Press, 1999.

[12] Xu, N., Ahuja, N., and Bansal, R., *"Automated Lung Nodule Segmentation Using Dynamic Programming and EM Based Classification",* Proceedings of SPIE , Medical Imaging 2002: Image Processing, Vol. 4684, pp. 666-676, May 2002.

[13] Sivakumar, S., and Chandrasekar, C., *"Lung Nodule Detection Using Fuzzy Clustering and Support Vector Machines",* International Journal of Engineering and Technology (IJET), Vol. 5, No. 1, pp. 179-185, Feb-Mar 2013.

[14] Azhari, E.M., Hatta, M.M.M., Htike, Z.Z., and Win, S.L., *"Brain Tumor Detection and Localization in Magnetic Resonance Imaging",* International Journal of Information Technology Convergence and Services (IJITCS), Vol. 4, No. 1, February 2014.

[15] Sachin N.G., Khairnar V., and Kadu S., *"Brain Tumor Detection Based on Mathematical Analysis and Symmetry Information",* International Journal of Engineering Research and Applications, Vol. 4, No. 2 (Version 1), pp. 231-235, February 2014.

[16] Selkar, R.G., and Thakare, M.N., *"Brain Tumor Detection and Segmentation by Using Thresholding and Watershed Algorithm",* International Journal of Advanced Information and Communication Technology (IJAICT), Vol. 1, No. 3, July 2014.

[17] Joseph, R.P., Singh, C.S., and Manikandan, M., *"Brain Tumor MRI Image Segmentation and Detection in Image Processing",* International Journal of Research in Engineering and Technology (IJRET), Vol. 3, No. 1 (special issue), pp. 1-5, March 2014.

[18] Mello, C.A.B., dos Santos, W.P., Rodrigues, M.A.B., Candeias, A.L.B., and Gusmao, C.M.G., *"Image Segmentation of Ovitraps for Automatic Counting of Aedes Aegypti Eggs",* 30th Annual International IEEE EMBS Conference Vancouver, British Columbia, Canada, pp. 3103-3106, August 2008.

[19] Guo, X., and Yu, F., *"A Method of Automatic Cell Counting Based on Microscopic Image",* 5th International Conference on Intelligent Human-Machine Systems and Cybernetics, China, Vol. 1, pp. 293-296, August 2013.

[20] Venkatalaksmi, B., and Thilagavathi, K., *"Automatic Red Blood Cell Counting Using Hough Transform",* Proceedings of 2013 IEEE Conference on Information and Communication Technology, pp. 267-271, April 2013.

[21] Fabic, J.N., Turla, I.E., Capacillo, J.A., David, L.T., and Naval, P.C., *"Fish Population Estimation and Species Classification from Underwater Video Sequences using Blob Counting and Shape Analysis,"* International Underwater Technology Symposium (UT), Japan, pp. 1- 6, March 2013.

[22] Pandit, A., and Rangole, J., *"Literature Review on Object Counting using Image Processing Techniques",* International Journal of Advanced Research in Electrical, Electronics and Instrumentation Engineering, Vol. 3, No. 4, April 2014.

[23] Bayram, B., *"Sayısal Görüntü İşleme",*
http://www.yildiz.edu.tr/~bayram/sgi/saygi.htm, [Visit Date: 05.04.2016].

[24] Young, I.T., Gerbrands, J.J., and van Vliet, L.J., *" Fundamentals of Image Processing",*
http://homepages.inf.ed.ac.uk/rbf/CVonline/LOCAL_COPIES/TUDELFT/FIP2_3.pdf, [Visit Date: 23.05.2015].

[25] İncetaş, M.O., *"Tıbbi Görüntülerin Uyarlanabilir Bölge Genişletme Algoritması ile Analizi",* Thesis (PhD), Gazi University, Institute of Science and Technology, Department of Industrial Technology Education, 2014.

[26] Jayaraman, S., Esakkirajan, S., and Veerakumar, T., *"Digital Image Processing",* Publisher: Tata McGraw - Hill Education Pvt. Ltd, New Delhi, Edition: 3, 2010.

[27] Wikipedia, *"Binary Image",* https://en.wikipedia.org/wiki/Binary_image, [Visit Date: 25.04.2014].

[28] Wikipedia, *"Grayscale"*, http://en.wikipedia.org/wiki/Grayscale, [Visit Date: 25.04.2014].

[29] Gopinath, N., *"Extraction of Cancer Cells from MRI Prostate Image Using MATLAB" ,* International Journal of Engineering Science and Innovative Technology (IJESIT), Vol. 1, No. 1, pp. 27-35, September 2012.

[30] Zhou, H., Wu, J., and Zhang, J., *"Digital Image Processing: Part I",* bookboon.com, 2010/a.

[31] Fisher, R. , Perkins, S. , Walker, A., and Wolfart, E.*,"Unsharp Filter",* http://homepages.inf.ed.ac.uk/rbf/HIPR2/unsharp.htm, [Visit Date: 26.06.2015].

[32] Patil, R.C., and Bhalchandra, A. S., *"Brain Tumour Extraction from MRI Images Using MATLAB",* International Journal of Electronics, Communication & Soft Computing Science and Engineering, Vol. 2, No. 1, April 2012.

[33] Dougherty, G., *"Digital Image Processing for Medical Applications",* Cambridge University Press, New York, 2009.

[34] Zhou, H., Wu, J., and Zhang, J., *"Digital Image Processing: Part II",* bookboon.com, 2010/b.

[35] Wismüller, A., Vietze, F., and Dersch, D.R., *"Segmentation with Neural Networks",* I.N. Bankman (ed.), Handbook of Medical Imaging, Processing and Analysis, Academic Press, San Diego, pp.107-126, 2000.

[36] Bankman, I.N., *"Segmentation, Handbook of Medical Imaging",* Academic Press, San Diego, pp. 67-68, 2000.

[37] Maraş, H.H., *"PC Tabanlı Üç Boyutlu Tıbbi Görüntü İşleme Uygulaması",* Thesis (M.Sc), Selçuk University, Institute of Science and Technology, Department of Computer Engineering, 2005.

[38] Uslu, Ü., *"Tomografik Görüntü Verilerinden 3 Boyutlu CAD Modellerinin Oluşturulması",* Thesis (M.Sc), Yıldız Teknik University, Institute of Science and Technology, Department of Mechanical Engineering, 2008.

[39] Patra, J., Manna, A.K., Moulick, H.N., Moulick, H.N., and Kumar, A., *"Segmentation Techniques Used Image Recognition and SAR Image Processing",* IOSR Journal of Computer Engineering (IOSR-JCE), Vol. 16, No. 2, pp. 37-43, 2014.

[40] Ruparelia, S., *"Implementation of Watershed Based Image Segmentation Algorithm in FPGA",* Thesis (M.Sc) (Nr. 3256), University of Stuttgart, Institute of Parallel and Distributed Systems, Department of Parallel Systems, 2012.

[41] Parkhedkar, S.R., and Dubey, Y.K., *"Brain Tumour Detection of MR Images Using Intuitionistic Fuzzy Sets*", IJCA Special Issue on International Conference on

Reliability, Infocom Technology and Optimization (ICRITO), pp. 30-35, August 2013.

[42] Solomon, C., and Breckon, T., *"Fundamentals of Digital Image Processing: A Practical Approach with Examples in Matlab",* Wiley-Blackwell, 2010.

[43] Barbedo, J.G.A., *"Automatic Object Counting in Neubaur Chamber"*, Proceedings of XXXI Brazilian Telecommunications Symposium, Fortaleza, Brazil, December 2013.

[44] *"Blob Analysis"*, http://docs.adaptive-vision.com/current/studio/machine_vision_guide/BlobAnalysis.html, [Visit Date: 16.10.2015].

[45] Sertel, O., *"BLOB Analysis (Introduction to Video and Image Processing) Part 1"*, http://what-when-how.com/introduction-to-video-and-image-processing/blob-analysis-introduction-to-video-and-image-processing-part-1/, [Visit Date: 16.10.2015].

[46] Hough, P.V.C., *"Machine Analysis of Bubble Chamber Pictures",* Proceedings of 2nd International Conference on High-Energy Accelerators and Instrumentation, Geneva, Switzerland, pp. 554-558, 1959.

[47] Ballard, D.H., *"Generalizing the Hough Transform to Detect Arbitrary Shapes",* Pattern Recognition, Vol. 13, No. 2, pp. 111–122, 1981.

[48] Leibe, B., Leonardis, A., and Schiele, B., *"Robust Object Detection with Interleaved Categorization and Segmentation",* International Journal of Computer Vision (IJCV), Vol. 77, No. 1-3, pp. 259–289, 2008.

[49] Maji, S., and Malik, J., *"Object Detection Using a Max-Margin Hough Tranform",* Conference on Computer Vision and Pattern Recognition (CVPR), Miami, FL, USA, pp. 1038–1045, 2009.

[50] Gall, J., and Lempitsky, V., *"Class-Specific Hough Forests for Object Detection",* Computer Vision and Pattern Recognition (CVPR), Miami, FL, USA, pp. 1022–1029, 2009.

[51] Gu, C., Lim, J. J., Arbelaez P., and Malik J., *"Recognition Using Regions",* Computer Vision and Pattern Recognition (CVPR), Miami, FL, USA, pp. 1030-1037, 2009.

[52] Okada, R., *"Discriminative Generalized Hough Transform for Object Detection",* 12th International Conference on Computer Vision (ICCV), pp. 2000–2005, 2009.

[53] Bourdev, L., and Malik, J., *"Poselets: Body Part Detectors Trained Using 3D Human Pose Annotations",* 12th International Conference on Computer Vision (ICCV), pp. 1365–1372, 2009.

[54] Barinova, O., Lempitsky, V., and Kohli, P., *"On Detection of Multiple Object Instances using Hough Transforms",* IEEE Transactions on Pattern Analysis and Machine Intelligence, Vol. 34, No. 9, pp. 1773-1784, 2012.

[55] Illingworth, J., and Kittler, J., *"A Survey of the Hough transform"* , Computer Vision, Graphics, and Image Processing, Vol. 44, pp. 87-116, August 1988.

[56] Reddy, V.H., *"Automatic Red Blood Cell and White Blood Cell Counting For Telemedicine System",* International Journal of Research in Advent Technology, Vol. 2, No. 1, pp. 294-299, January 2014.

[57] Tangsuksant, W., Pintavirooj, C., Taertulakarn, S., and Daochai, S., *"Development Algorithm to Count Blood Cells in Urine Sediment using ANN and Hough Transform",* 6th Biomedical Engineering International Conference, Thailand, pp. 1-4, October 2013.

[58] Wikipedia, *"Connected-component labeling",* https://en.wikipedia.org/wiki/Connected-component_labeling, [Visit Date: 16.10.2015].

[59] Shaik A.R., *"Image Processing Technique to Count The Number of Logs in a Timber Truck",*
http://www.idt.mdh.se/kurser/ct3340/ht11/MINICONFERENCE/FinalPapers/ircse11_submission_10.pdf, [Visit Date: 22.10.2015].

[60] Dimitriou, M., Kounalakis, T., Vidakis, N., and Triantafyllidis, G., *"Detection and Classification of Multiple Objects using an RGB-D Sensor and Linear Spatial Pyramid Matching",* Electronic Letters on Computer Vision and Image Analysis, Vol. 12, No. 2, pp. 78-87, 2013.

[61] Halgaonkar P.S., *"Connected Component Analysis and Change Detection for Images",* International Journal of Computer Trends and Technology, Vol. 1, No. 2, pp. 224-227, 2011.

[62] Barbedo, J.G.A., *"Method for Counting Microorganisms and Colonies in Microscopic Images",* 12th International Conference on Computational Science and Its Applications (ICCSA), Brazil, pp. 83-87, June 2012.

[63] Ramin, M., Ahmadvand, P., Sepas-Moghaddam, A., and Dehshibi, M.M., *"Counting Number of Cells in Immunocytochemical Images using Genetic Algorithm",* 12th International Conference on Hybrid Intelligent Systems, India, pp. 185-190, December 2012.

[64] Vikipedi, *"Görüntüleme Yöntemleri ve Ana Prensipler",* https://tr.wikipedia.org/wiki/Görüntüleme_Yöntemleri_ve_Ana_Prensipler, [Visit Date: 15.12.2015].

[65] Yazgan, E., *"Tıbbi Görüntüleme Teknikleri",* Elektrik Mühendisliği Dergisi, Biyomedikal özel sayısı, Vol. 38, No. 390, pp. 341-357, 1993.

[66] "İleri Görüntüleme Yöntemleri", www.dentistry.ankara.edu.tr/ders/odr-sg-05.doc, [Visit Date: 15.12.2015].

[67] Ünal, D., *"Tıpta Kullanılan Görüntüleme Teknikleri",* Thesis (M.Sc), Gazi University, Faculty of Education, Department of Physics Education, Ankara, 2008.

[68] http://www.tibbiterminoloji.com/home/bilgisayarli-tomografinin-tarihsel-gelisimi, [Visit Date: 15.12.2015].

[69] İnal, T., *"X-Işını Bilgisayarlı Tomografisi (Computed Tomography-Ct) Tek ve Çok-Kesitli Sistemlerde Kalite Kontrol Testlerinin Standartizasyonu",* Thesis (M.Sc), Ankara University, Institute of Science and Technology, Department of Physics Engineering, 2007.

[70] Kalender, W.A., *"Computed Tomography Fundamentals System Technology, Image Quality, Applications",* Publicis MCD Verlag, 218, Germany, 2000.

[71] Kılıç, N., *"Bilgisayarlı Tomografi Görüntülerde Üç Boyutlu Şablonlar Kullanılarak Kolonik Polip Tespiti",* Thesis (PhD), İstanbul University, Institute of Science and Technology, 2008.

[72] Wikipedia, *"Hounsfield Scale",*
https://en.wikipedia.org/wiki/Hounsfield_scale, [Visit Date: 01.05.2016].

[73] Akın, K., *"Bilgisayarlı Tomografi Fiziği",*
http://slideplayer.biz.tr/slide/2001240/#, [Visit Date: 15.12.2015].

[74] Millî Eğitim Bakanlığı, *"Bilgisayarlı Tomografi Cihazları",* Radyoloji, Ankara, 2011.

[75] Lifemed, *"Bilgisayarlı Tomografi (BT) Yaptırmanın Avantajları?",* http://www.lifemed.com.tr/bilgisayarli-tomografi/bilgisayarli-tomografi-bt yaptirmanin-avantajlari/, [Visit Date: 03.05.2016].

[76] Lifemed, *"Bilgisayarlı Tomografi (BT) Zararları Nelerdir?",* http://www.lifemed.com.tr/bilgisayarli-tomografi/bilgisayarli-tomografi-bt-zararlari-nelerdir/ , [Visit Date: 03.05.2016].

[77] Wikipedia, *"Computer-aided diagnosis",* https://en.wikipedia.org/wiki/Computer-aided_diagnosis, [Visit Date: 17.12.2015].

[78] El-Dahshan, S.A., Mohsen, H.M. , Revett, K., and Salem, M., *"Computer-aided Diagnosis of Human Brain Tumor Through MRI: A Survey and a New Algorithm",* Elsevier Journal, Vol. 4, No. 11, pp. 5526–5545, September 2014.

[79] Clarke, L.P, Croft, B.Y, Staab, E., Baker, H., and Sullivan, D.C, *"National Cancer Institute Initiative",* Academic Radiology Journal, Vol. 8, No. 5, pp. 447-450, May 2001.

[80] Halezeroğlu, S., *"Akciğer Nodülü Nedir?",* http://www.akcigercerrahisi.com/akcigerde-nodul-ne-yapmali/, [Visit Date: 17.12.2015].

[81] akciger.gen.tr, *"Akciğerde Nodül",* http://www.akciger.gen.tr/akcigerde-nodul.html, [Visit Date: 17.12.2015].

[82] Grove, O., Berglund, A.E., Schabath, M.B., Aerts, H.J.W.L., Dekker, A., Wang, H., Velazquez, E.R., Lambin, P., Gu, Y., Balagurunathan, Y., Eikman, E., Gatenby, R.A., Eschrich, S., and Gillies, R.J., *"Quantitative Computed Tomographic Descriptors Associate Tumor Shape Complexity and Intratumor Heterogeneity with Prognosis in Lung Adenocarcinoma",* http://journals.plos.org/plosone/article?id=10.1371/journal.pone.0118261, [Visit Date: 16.05.2016].

[83] *"The Cancer Imaging Archive (TCIA)",* https://wiki.cancerimagingarchive.net/display/Public/LungCT-Diagnosis, [Visit Date: 16.05.2016].

BIOGRAPHY

Zeynep Yıldız was born in Ankara, Turkey in 1989. She was graduated from Süleyman Demirel University, Isparta in 2012. Her department was Electronics and Communication Engineering. Then she started master education in Yıldırım Beyazıt University, Ankara. Her main areas of research interest are signal processing, image processing and analysis, biomedical image processing and analysis.